HYMEPRO

Hybrid Membrane Process for Water Treatment
Project Report
1.9.2011 – 31.12.2014

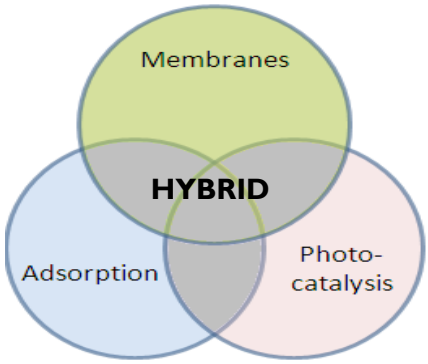

UNIVERSITY of OULU
OULUN YLIOPISTO

CONTENTS

1 INTRODUCTION

Background

Water has a major role in the wellbeing of all humans, however, over 760 million people do not have access to safe, and clean drinking water. Arsenic in particular is a global problem since over 130 million people are exposed to levels of arsenic in drinking water above the World Health Organization's drinking water standard. Therefore, water contamination is today a major problem globally and the growing utilization of limited water resources creates a need for efficient purification methods.

Industrial water treatment is important, since industrial effluents are often discharged straight into the environment and the contaminants may end up in fresh water sources such as rivers, lakes and ground water, especially in developing countries where people are consuming these waters without any purification. On the other hand, companies are increasingly being forced both by regulatory and cost pressures to reduce the amount of waste they produce and the hazard it places on the environment. The purification of wastewater minimizes wastewater volumes and reduces the harm towards human beings and the environment by eliminating the discharges of harmful compounds, improving the resource efficiency of valuable compounds and promoting water re-use and thus reducing the freshwater consumption.

One specific problem existing in the mining and metallurgical industries is the need for more efficient treatment technologies for the removal of metals and nutrients from wastewaters. Nutrients, such as nitrates, are also valuable compounds for example for fertilizer industry. In addition, the European Union has launched a thematic strategy on the sustainable use of natural resources with the aim to reduce the depletion and pollution of natural resources, such as water, in a growing economy. Therefore, there is a substantial need for innovative environmental technologies and clean, cost-effective, sustainable industrial processes to meet the global efforts on combating pollution.

The increased demands for both drinking water quality and industrial effluents encourage the development of effective and low cost water treatment technologies. One possibility for achieving this aim is to combine existing methods into a so-called hybrid process. Generally, hybrid processes have been described as processes where one or more processes are coupled with other unit process and are integrated into a single system. Several different physical, chemical and/or biological processes can be combined so that they complement each other well, thus forming a hybrid process. This way, the disadvantages of each separated process can be overcome and the advantages can be further enhanced and hence the sustainability and process efficiency can be improved.

Objectives

The main objective of this project was to develop a hybrid membrane reactor for innovative water treatment using membrane technology, photocatalysis and adsorption. The developed technique aimed to simultaneous removal of pollutants and recovery of valuable compounds eco-efficiently from wastewaters. The main input and collaboration of the research partners is presented in Fig. 1.

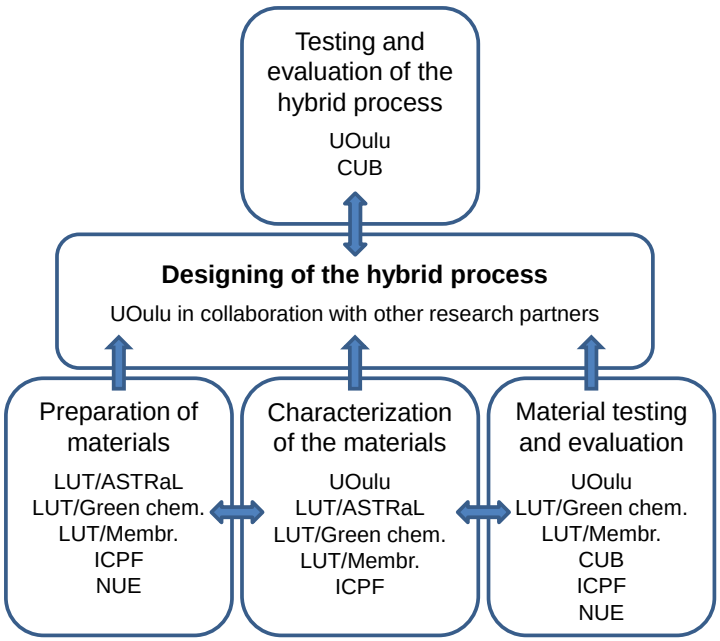

Figure 1 Main input and collaboration of the research partners.

The tasks of the project:

- To develop a hybrid membrane process for more efficient water treatment.
- To apply developed materials for simultaneous purification, degradation, concentration and separation of different pollutants.
- To develop novel membranes with enhanced functionalities; robust, safe and efficient membranes.
- To use visible LED-light for improved energy efficiency of the process.
- To foster networking between material producers/suppliers, water treatment facilities providers, end users.
- To enhance resource efficiency by converting waste into valuable compounds.

2 CONSORTIUM

Research consortium:

1. University of Oulu, Faculty of Technology, Environmental and Chemical Engineering Research Group (ECE), (Previously Mass and Heat Transfer Process Laboratory /MHTPL), Prof. Riitta Keiski (UOulu)
2. Lappeenranta University of Technology,
   a. Advanced Surface Technology Research Laboratory, Prof. David Cameron (LUT/ASTRaL)
   b. Laboratory of Membrane Technologies, Prof. Mika Mänttäri (LUT/membrane)
   c. Laboratory of Green Chemistry, Prof. Mika Sillanpää (LUT/LGC)

International research partners:

1. Corvinus University of Budapest, Department of Food Engineering, Hungary, Prof. Gyula Vatai (CUB)
2. Institute of Chemical Process Fundamentals of the Academy of Sciences of the Czech Republic, v.v.i., Department of Catalysis and Reaction Engineering, Dr. Olga Šolcová (ICPF)
3. National University of Engineering, (Universidad Nacional de Ingenería, UNI) Lima, Peru, Science Faculty, Functional Materials Laboratory, Assoc. Prof. José Solís Veliz

Industrial partners:

1. Agnico-Eagle Finland Oy
2. Aquator Oy,
3. Beneq Oy
4. Envitop Oy
5. Honkajoki Oy
6. Kemira Oyj
7. Miktech Oy
8. Outokumpu Stainless Oyj
9. Outotec Oyj
10. Sachtleben Pigments Oy
11. Talvivaaran Kaivososakeyhtiö Oyj
12. Watman Engineering Ltd Oy

Other international collaboration:

1. National University of Tumbes (Universidad Nacional de Tumbes), Departamento Académico de Ingeniería Forestal y Gestión Ambien, Tumbes, Peru. Dr. Gerardo Cruz
2. University of Cantabria, Department of Chemical Engineering and Inorganic Chemistry, Santander, Spain. Prof. I. Ortiz
3. Institute of Chemical Technology, Department of Chemical Engineering, Mumbai, India. Prof. G.D. Yadav
4. University of Chouaïb Doukkali, El Jadida, Morocco. Prof. R. Brahmi

Contact information

Responsible leader of the project:

Professor Riitta Keiski, riitta.keiski@oulu.fi, +358 29 448 2348

Project coordinator:

Minna Pirilä, minna.pirila@oulu.fi, +358 29 448 2387

Contact person in Lappeenranta University of Technology:

Professor Mika Mänttäri, mika.manttari@lut.fi, +358 40 734 2192

3 GREETINGS FROM INDUSTRY – TALVIVAARA MINING COMPANY PLC.

The research of new processes is essential to develop possibilities to gain better results in environmentally important issues. Industrially feasible water purification techniques should be simple and straightforward.

In this project all the project parties have received valuable information and new knowledge on industrial wastewater treatment via membrane techniques, adsorption and photocatalysis and their combinations.

We have seen progress in developing the known water purification techniques to new possibilities. The hybrid techniques tested were challenging but gave new ideas towards the future. There has also been taken a step in improving the old techniques to be more efficient and feasible to industry in the future.

This will encourage industry to continue the R&D activities also in new projects in this area.

Talvivaara is highly interested in the development of membrane techniques and also possibilities with new adsorbent materials are welcome.

Talvivaara 16.4.2015
Ville Heikkinen
Manager
Production development
Talvivaara Mining Company Plc.

4 UNIVERSITY OF OULU (UOULU)

Environmental and Chemical Engineering Research Group (previously Mass and Heat Transfer Process Engineering)

Minna Pirilä, Piia Häyrynen, Kaisu Ainassaari, Paula Saavalainen, Hanna Valkama, Junkal Landaburu-Aguirre, Ritva Lenkkeri, Kirsi Ahtinen, Buddhika Rathnayake, Prem Seelam, Mika Huuhtanen, and Prof. Riitta L. Keiski

Prof. Riitta Keiski
Supervisor
Responsible leader

Minna Pirilä
Researcher
Coordinator

Piia Häyrynen
Researcher

Kaisu Ainassaari
Researcher

Hanna Valkama
Researcher

Paula Saavalainen
Researcher

Junkal Landaburu
Researcher

Ritva Lenkkeri
Researcher

Liisa Myllykoski
Economic issues

Kirsi Ahtinen
Laboratory assistant

Mika Huuhtanen
Advisor

University of Oulu, Faculty of Technology,
P.O. Box 4600,
FI-90014 University of Oulu

Abstract

The role of the Environmental and Chemical Engineering Research Group in HYMEPRO project was to study different water treatment techniques including membrane techniques, adsorption and photocatalysis, first separately. After gaining information from the separate methods, the aim was to develop a hybrid method by combining the previous methods together. The developed hybrid method contains only membrane technique (nano- or ultrafiltration) and photocatalysis, however, adsorption can be used as an additional water treatment step before or after the hybrid process. In the hybrid method, photocatalytic material was added on the membrane surface by atomic layer deposition, done in the LUT/ASTRaL.

International collaboration has been active within the whole project period with all the international partners. For example, with Peruvian research partners the adsorption material development has been very fruitful, the partners from Czech Republic have contributed a lot to the material characterization, and with Hungarian partners the research included membrane distillation and reverse osmosis for the concentration of heavy metals.

Introduction

More than 600 organic and inorganic pollutants have been reported in water along with biological pollutants (Gupta & Ali 2013). Among these pollutants, toxic heavy metals and metalloids as well as organic pollutants are a serious concern for human health and the environment. Moreover, metal ions are not biodegradable or bio-transformable and, hence, exist in the environment for long time. These contaminants are present, for example, in drinking water sources as well as in industrial waste streams, and must be controlled to an acceptable level according to environmental regulations worldwide.

Traditional methods for the wastewater treatment are e.g. precipitation, ion exchange, electrodeposition, crystallization, evaporation and liquid-liquid extraction. Some of these processes have a great disadvantage of using heterogeneous reactions or distributions of substances among different phases, which are phenomena controlled by diffusion and thus requiring usually large operating times. In other cases, traditional techniques do not work on dilute systems, and the side-product of the process creates a new waste management problem. When merging separate process units into one hybrid process disadvantages of each process can be overcome and in that way sustainability and process efficiency can be improved (Mavrov et al. (2003).

Membrane technology and photocatalysis can be combined into a hybrid process by adding a photocatalytic coating layer on the membrane surface. The coating layer should decrease membrane fouling since the organic compounds which will build up on the membrane surface will be degraded into smaller compounds by photocatalysis. Also permeate quality and energy efficiency are noticed to be improved with photocatalytic membranes. (Leong et al. 2014)

The work of Environmental and Chemical Engineering research group in the HYMEPRO project has been done in close co-operation with other projects: (1) Design of adsorption materials and units for water treatment for rural Peruvian areas - Use of activated carbon obtained from domestic agricultural materials (AdMatU/Academy of Finland); (2) Advanced Oxidation Processes for Industrial Wastewater Treatment (AOPI/Academy of Finland); (3) Implementation of highly efficient TiO_2 based photocatalyst nanomaterials (ImPhoNa/Tekes); (4) Sulphur Compounds in Mining Operations – Environmental Impact Assessment, Measurement and Emission Abatement (Sulka/European Regional Development Fund); (5) The applications of green technologies for sustainable water purification and reuse (GreenTech/New Indigo ERA-NET NPP2 -programme); and (6) Utilization of industrial By-products and Waste in Environmental Protection (NO-WAST /FP7 Marie Curie Actions).

Objectives of the research

- Experiments for arsenic, heavy metals and nutrients removal for the design of the hybrid process.
- Testing and selection of membranes, adsorbents and photocatalysts.
- Concentration of nitrates by membrane techniques and oxidation studies of nitrites to nitrates by photocatalysis.
- Testing of catalytic membranes obtained from other research groups.
- Design and set-up of a hybrid reactor in cooperation with the project partners.
- Experiments using the hybrid reactor.
- Sustainability evaluation of the developed hybrid process using sustainability assessment analysis as a tool.
- Providing information and knowledge for other research groups.

Materials and methods

Membrane and hybrid membrane experiments

Equipment

The nanofiltration experiments were mainly carried out in Sepa CF II cross-flow filtration unit manufactured by GE Osmonics (Figure 1). The active membrane area of the membrane cell was 0.014 m^2. The pump used was a Wanner Hydra-Cell WG-03 diaphragm pump.

The photocatalytic membrane unit was built during the project (Figure 1 a). In the photocatalytic membrane cell flat sheet membranes (active membrane area 0.014 m^2) were tested. The feed side of the membrane was irradiated with 20 UV-A led lamps. The maximum pressure of the cell is approximately 10 bars and the illuminated membrane area is 0.010 m^2. The operational principle of the photocatalytic membrane cell is shown in Figure 1 b.

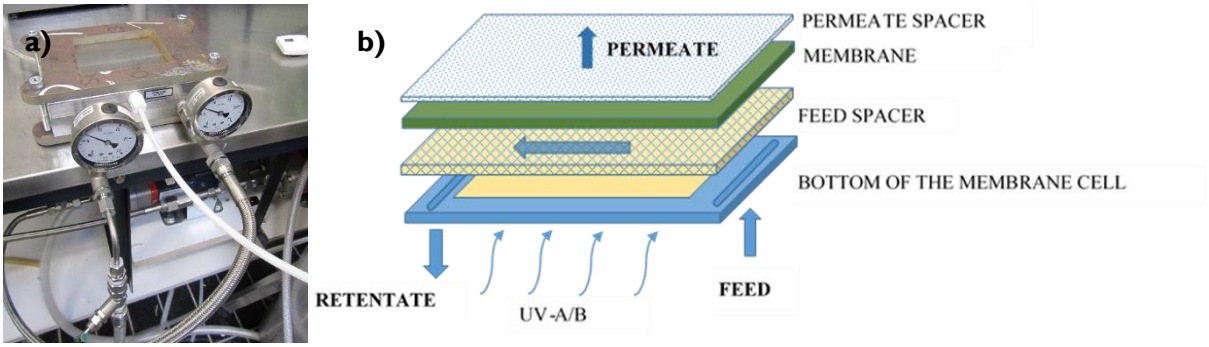

Figure 1 Photocatalytic membrane cell (a) and its operating principle (b).

The initial permeate flux was measured prior to each experiment using deionized water. The experiments were conducted in a complete recycle mode, meaning that the retentate and permeate streams were recycled back to the feed tank. The reactor temperature was kept constant at 21 ± 1°C to avoid changes in the permeate flux.

Tested commercial membranes

Nanofiltration membranes NF90 and NF270 by Dow Filmtec were used as commercial membranes in the experiments. Characteristics of the membranes are represented in Table 1. NF90 and NF270 are polymeric composite polyamine and polypiperazine thin-film composite nanofiltration membranes, respectively. The molecular weight cut off (MWCO) of NF90 is 100-200 Da and it is recommended for the removal of salts, nitrate, iron and organic compounds. NF270 is designed for the total organic compounds' removal and it has a medium to high salt and medium hardness passage having MWCO of 150-300 Da.

Table 1 Characteristics of the NF90 and NF270 membranes.

	NF90	**NF270**
Membrane material	Polyamine thin-film composite	Polypiperazine thin-film composite
Molecular weight cut-off	100-200 Da	150-300 Da
Max. operating pressure	41 bar	41 bar
pH range	3-10	3-10
Max. temperature	45 °C	45 °C

Tested coated membranes

The commercial nanofiltration membranes presented in Table 1 were coated with a ZnO photocatalyst by atomic layer deposition (ALD) technique. The membranes were coated by LUT in Mikkeli. The coating thicknesses were 10 and 20 nm. Since polymeric membranes do not tolerate high temperatures during the coating processes, the membranes were calcined below 120 °C.

The results of the coated membranes were compared to commercial membranes without the coating layer. The coated membranes were used without UV-light in the mine wastewater treatment and with UV-light for bisphenol-A removal and degradation.

Analyses

Heavy metal concentrations were analysed with an ICP-OES analyser. Conductivity and pH of the water samples were measured during the filtration experiments. Nitrate concentrations were analysed with a flow injection analyser and a spectrophotometer was used for the analysis of organic compounds.

Wastewaters

The real wastewaters were prefiltered with the Millipore Polygard 0.45µm cartridge filter to remove colloidal particles and to reduce membrane fouling during experiments. If pH was above 10, it was decreased with HNO_3 to pH 8.

Calculations

The membrane process performance was evaluated by means of permeate flux and rejection coefficients. The permeate flux was measured in each experiment before, during and after each experiment. The permeate flux was calculated using Equation (1)

$$J = \frac{V}{At} \quad (1)$$

where J is the permeate flux [L/m$_2$H], V is the permeate volume [L], A is the active membrane area [m^2] and t is time [h].

Rejection coefficients were calculated for sulphate and other compounds. The rejection coefficient was calculated with Equation (2)

$$R(\%) = \left(1 - \frac{C_{Pi}}{C_{Ri}}\right) * 100 \quad (2)$$

where R is the rejection coefficient [%], C_{Pi} is the concentration of compound i in the permeate stream [mg/L] and C_{Ri} is the concentration of compound i in the retentate stream [mg/L].

Adsorption experiments

Equipment

Adsorption experiments were carried out in two experimental setups. The kinetic experiments and adsorption capacity experiments were done as batch experiments in Erlenmeyer flasks mixed by a mechanical shaker. In methylene blue experiment the concentration of MB was 50 mg/l, and the mass concentration of the adsorbent was 1 g/l. In arsenic removal experiments the concentration of As was 100 μg/l and the mass concentration of the adsorbent was 0,5 g/l. The pH of the solution was set to 6 in the beginning of the experiments with dilute NaOH.

In fixed-bed column experiments the synthetic wastewater containing 1000 μg/l As(V) and Cd(II), and 500 μg/l Cr(III) and Ni(II) flew from the solution bucket through the column bed (up flow mode). The pH of the feed solution was 3.3. The duration of the experiment was 2 months.

Adsorbents

In the mechanical shaker experiments for As removal there were 5 adsorbents: adsorbent sample obtained from Kemira, three activated carbons prepared from Peruvian agrowastes MSIP (mango seed internal part), Corn cop and CPH (cocoa pod husk), and a commercial activated carbon ChemViron. In MB experiments there were four activated carbons prepared from cocoa pod husk (CPH) with different activation methods, two different Finnish pine wood gasification activated carbons (GAS), Finnish pine wood pyrolysis activated carbon (PAC), sugarcane pyrolysis waste and commercial activated carbon ChemViron.

In the fixed-bed column experiments the adsorbents used were industrial side product granules Sachtofer PR from Huntsman Pigments and Additives (previously Sachtleben Pigments), commercial activated carbon and ash granules prepared by the Chemistry Department, University of Oulu.

Analyses

The MB concentration was determined by a UV-Vis spectrophotometer (Beckman DU-640i) at the wavelength of 660 nm. Heavy metal concentrations were analysed using an ICP-OES analyser.

Figure 2 Adsorption experiments in a mechanical shaker and in fixed-bed columns.

Photocatalytic experiments

Equipment

Photocatalytic experiments were carried out in two different self-constructed laboratory scale reactors, one made of quartz (1.0 l) (Fig. 3.) and the other made of Teflon with an inner glass cylinder for the test solution (0.5 l) (Fig. 4). Before the photocatalytic experiment, a 30 min dark period was used to establish the adsorption/desorption equilibrium between the solid and liquid materials in the reactors. After the dark period, the UV-A lamps were switched on. The temperature of the test solution was adjusted to room temperature during the experiment and followed with a thermocouple (Delta OHM HD2128.1). Samples were drawn at certain time intervals and filtered through a 0.2 µm filter (Millipore) to remove suspended TiO_2. The concentration of the pollutants, pH and TOC were measured from the filtered samples.

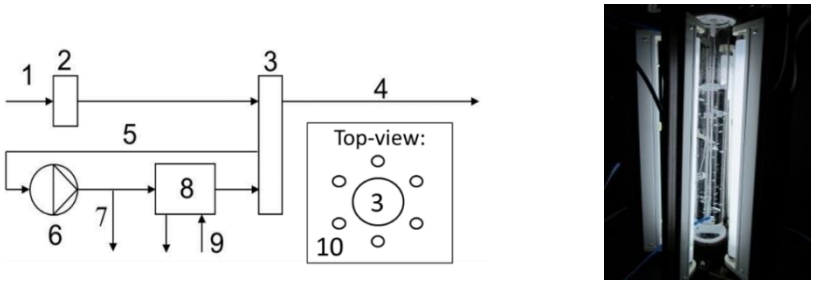

Figure 3 The photocatalytic Quartz reactor setup with 1 air flow inlet, 2 mass flow controller, 3 photoreactor, 4 gas outlet, 5 cooling circulation, 6 hose pump, 7 sampling, 8 heat exchanger, 9 cooling water in/out, 10 six UV-A lamps.

The quartz reactor was a vertical tubular reactor with a circulation loop. The circulation of the slurry was maintained by a peristaltic pump operating at a speed of 60 l/h. A synthetic air flow (6.5 cm^3s^{-1}) to the reactor was accomplished with a sintered glass tube to improve the dissolution of gas in the reaction suspension. The compartment contained six UV-A lamps with the maximum radiation at the wavelength of 365 nm (Philips, 15 W) which were placed outside the reactor hexagonally.

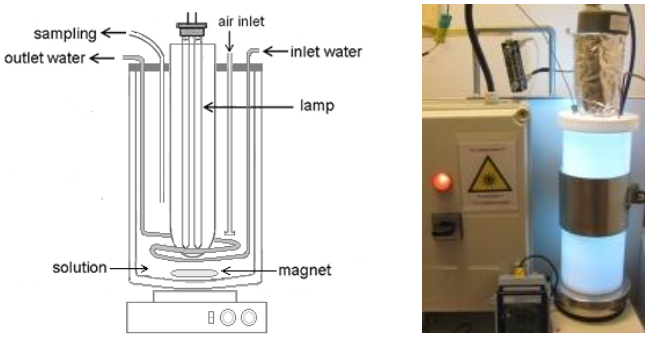

Figure 4 The experimental setup of the photocatalytic Teflon reactor.

The Teflon reactor was an annular type vertical batch photoreactor. Synthetic air was bubbled into the reactor with a flow rate of 2.5 cm^3s^{-1} before starting and during the experiments. The reactor had a plunging tube made of quartz and fixed in the middle of the reactor cell for the UV-A lamp. Constant agitation of the test solution was provided by a magnetic stirrer with approximately 250 rpm.

Organic pollutants

The photocatalytic degradation of four organic pollutants originating from different types of industry was studied both in synthetic solutions and in a diluted pharmaceutical industry wastewater matrix. The pollutants were Diuron (pesticide), *p*-Coumaric acid (PCOU) (agro-industrial wastewaters), bisphenol A (BPA) and phthalic anhydride (PHA) (plasticizers) (Fig. 5), which all are widely used and cause water contamination and further significant health and environmental problems.

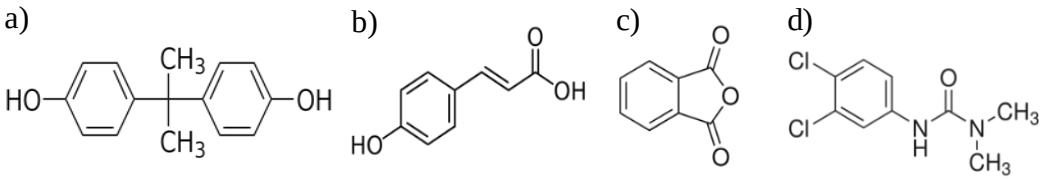

Figure 5 Molecular structures of the model compounds a) BPA, b) PCOU, c) PHA and d) Diuron (Pirilä et al. 2015).

The experiments were done with the initial concentration of 15 mg/l of the pollutants and with a catalyst dose of 200 mg/l. The pharmaceutical wastewater contained different organic compounds, mainly ethanol and smaller amounts of other alcohols and ketones. It was highly alkaline with a pH above 12. The total organic compound (TOC) content was 7600 mg l^{-1}. The actual test water was prepared by mixing 15 ml of industrial wastewater with 15 mg of each of the model compounds and by diluting the solution into 1000 ml with distilled water.

The studied photocatalyst was a commercial photoactive titanium dioxide, Aeroxide P25, and its characterized properties are shown in Table 2. The studied TiO_2 catalyst consists of mesoporous particles with an average pore size of approximately 7 nm and has a combination of both anatase and rutile phases. In the experiments with mine wastewater, Aeroxide P25 and Hombitan S141 photocatalysts were used for the oxidation of nitrogen compounds.

Table 2 Properties of the studied commercial Aeroxide P25 (Pirilä et al. 2015).

Property	Value
Crystal form	Anatase 82 wt%, rutile 18 wt%
S_{BET}	50 m^2/g
Pore volume	0.096 cm^3/g
Average pore width	7.2 nm

Mine wastewater

Mine wastewater containing nitrogen compounds was oxidised in photocatalysis experiments. The removal/oxidation of nitrate, nitirite and ammonium was studied. The mine wastewater contained also other ions such as sulphates considerable amounts.

Analyses

The concentration of the model pollutants were followed by a spectrophotometer (Beckman DU-640i) at the wavelengths of 228, 230, 248 and 283 nm for bisphenol A (BPA), phathalic anhydride (PHA), Diuron and *p*-Coumaric acid (PCOU), respectively.

Hybrid adsorption material development

The experimental goal was to obtain a hybrid material by adding a layer of semiconductor TiO_2 onto the surface of industrial side product granules Sachtofer PR (from Huntsman Pigments and Additives, previously Sachtleben Pigments Oy, Pori). These side-products were found to be adsorbing heavy metals and metalloids, and by adding a photocatalyst layer on the surface, a material with hybrid properties working both as an adsorbent and a photocatalyst could be achieved. The coating of the Sachtofer was done by dip-coating using TiO_2 precursor solutions (titanium(IV) isopropoxide, (97 %) 0.01–0.5 M) and 10 wt% TiO_2 photocatalyst powder (Degussa P25 and Hombicat UV100) suspensions. The coated materials were characterized by different methods and tested for the removal of the organic model compound methylene blue both by photocatalysis and adsorption.

Sustainability analysis

Quantitative and qualitative sustainability assessment methods were used to assess arsenic removal by adsorption. Adsorption is widely used for the removal of arsenic and so it was considered for the adsorption step. In the adsorption case different adsorbents were compared such as activated alumina (AA), iron impregnated granular activated carbon (Fe-GAC) and activated alumina including regeneration (AA-Reg). (Saavalainen et al. 2013)

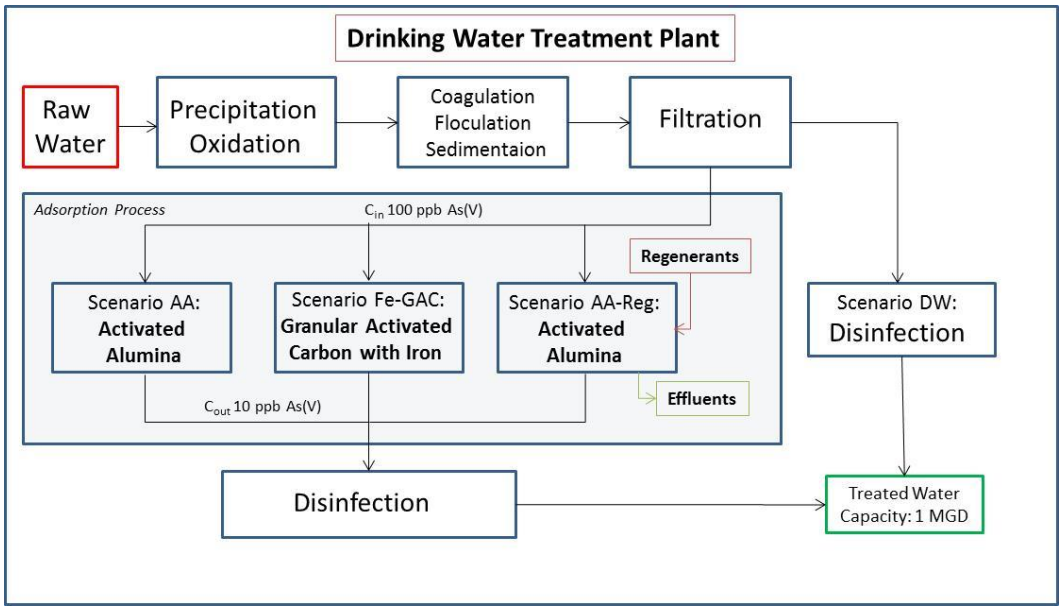

Figure 6 Scenarions for the research (Saavalainen et al. 2013).

Qualitative method

The qualitative method of sustainability assessment is completed by answering a creatively developed questionnaire which takes the most relevant information regarding sustainability into consideration. It focuses on the key aspects dealing with sustainability and evaluates the technology based on a score system. The sustainability assessment questionnaire is based on the twelve principles of Green Chemistry and is categorized as environmental, social and economic based on the process information available. (Saavalainen et al. 2013)

Quantitative method

Lifecycle approach (Fig. 7) was used to evaluate the environmental sustainability assessment (ESA) of the adsorption process for the removal of arsenic from 100 ppb to 10 ppb using adsorbents: activated alumina (AA) and iron impregnated granular activated carbon (Fe-GAC). The lifecycle inventory for the G-G step (Gate to Gate) was obtained by modelling and simulation of the adsorption process using the Langmuir isotherm parameters. (Saavalainen et al. 2013)

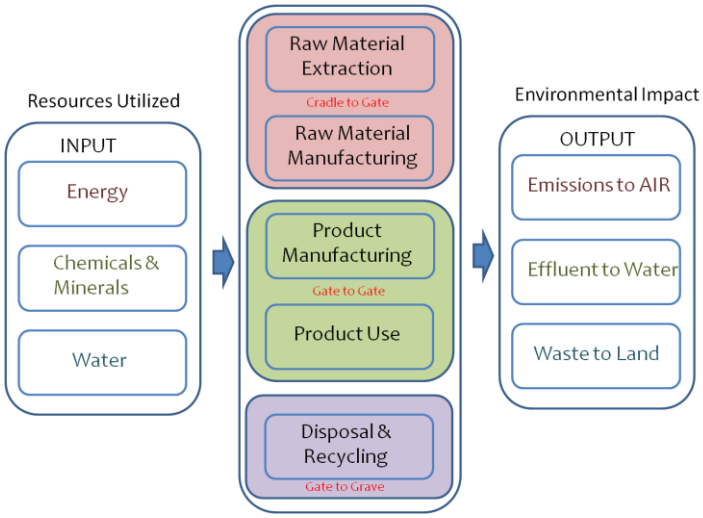

Figure 7 Schematic of LCIA Lifecycle Impact Assessment methodology (Chavan et al. 2015).

Results

Membrane experiments

Coated and commercial nanofiltration membranes were tested for the mine wastewater treatment. Pressure applied varied from 8 to 15 bar while the feed flow rate was constant. Rejection efficiencies and permeate fluxes were compared between coated and commercial membranes. It can be observed that the highest rejection efficiency was achieved with the NF90 membrane (Table 3 and 4). That is due to a smaller pore size of the membrane compared to NF270. As can be observed from Tables 3 and 4, the rejection coefficients vary depending on the compounds and on the mine wastewater.

For nitrogen compounds a negative rejection was observed. The negative rejection decreased at higher operating pressure. Also the high ionic strength of the solutions increases the possibility of negative rejection during nanofiltration processes. (Van der Bruggen et al. 2008)

The ZnO membrane coating increased the removal of sulphate ions, however the nitrate and chloride ion removal decreased compared to the uncoated membrane. According to the conductivity measurements, the removal efficiency of coated membranes compared to commercial ones varied and therefore the efficiency of the coated membranes need more studies.

Table 3 Mine wastewater 1: removal efficiency of ions by coated and commercial nanofiltration membranes at 8 and 15 bar.

8 bar				**15 bar**		
	NF270	**NF270 coated**	**NF90**	**NF270**	**NF270 coated**	**NF90**
SO_4^{2-}	91.06	93.51	99.49	92.63	96.77	99.58
NO_3	-43.17	-74.75	60.82	-	-	-
Cl^-	36.43	18.75	91.07	-	-	-
Conductivity	85.97	85.21	98.91	90.78	93.18	99.20

Table 4 Mine wastewater 2: removal efficiency of ions by coated and commercial nanofiltration membranes at 8 and 15 bar.

8 bar				15 bar		
	NF270	**NF270 coated**	**NF90**	**NF270**	**NF270 coated**	**NF90**
SO_4^{2-}	99.51	99.55	99.51	-	99.55	99.57
NO_3^-	28.75	21.28	70.95	-	-	-
Cl^-	56.42	57.23	90.56	-	-	-
Conductivity	93.23	94.17	100.00	-	95.29	100.00

Coating depletion occurred during the experiments. The Zn concentration was analysed and it was observed that Zn ions were released into permeate and retentate samples since the Zn concentration was increasing in the samples. Also in microscopic pictures (Fig 8 a and b) coating depletion was seen.

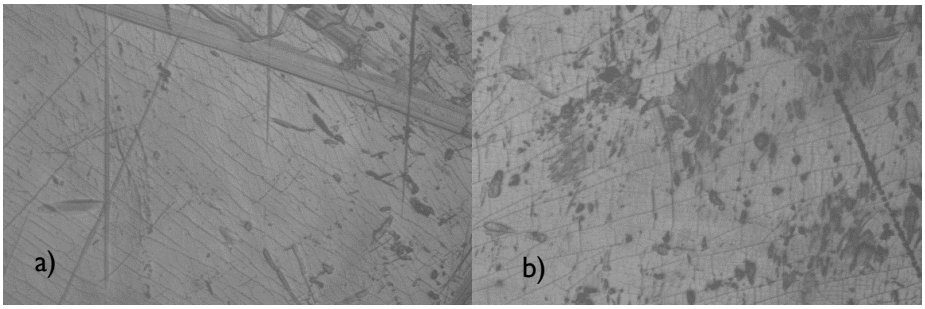

Figure 8 Coated membrane surface layer before (a) and after (b) filtration experiment.

The permeate flux was the highest for the NF270 membrane with and without the coating layer. NF90 had a lower permeate flux due to the smaller pore size. Figure 9 represents permeate fluxes of NF90, NF270 and coated NF270 membranes during the filtration experiments with the mine wastewater 1.

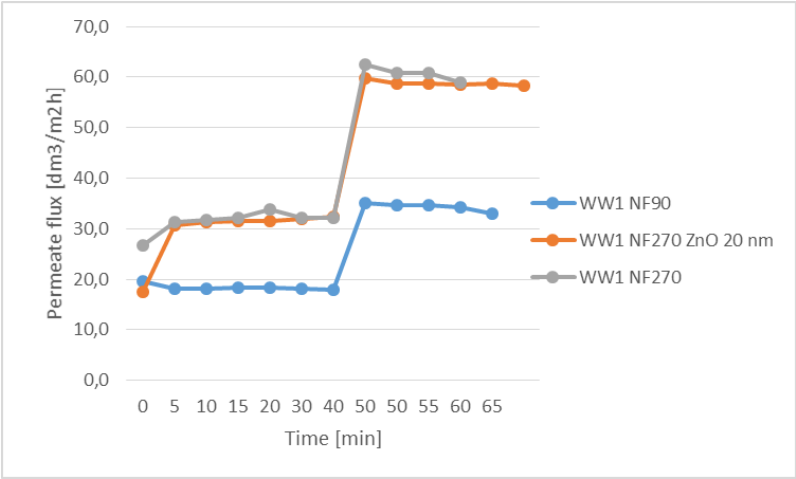

Figure 9 Permeate flux of NF90, NF270 and ZnO coated NF270 membranes in wastewater 1 filtration.

Adsorption experiments

In methylene blue adsorption experiments shown in Figure 10 the adsorbent prepared of cocoa pod husk (activation with $ZnCl_2$ at 650˚C, particle size <0.25 mm) turned out to be the most efficient adsorbent. The removal of MB reached almost 100% during the first 2 h of the experiment. Activation by $ZnCl_2$ gives the highest BET surface area, highest pore volume and the lowest ash content to the adsorbent (Cruz et. al. 2012). The particle size of the adsorbent plays also an important role in the removal efficiency of MB. Also several other prepared adsorbents were competitive with the commercial adsorbent after 22 h of experiment.

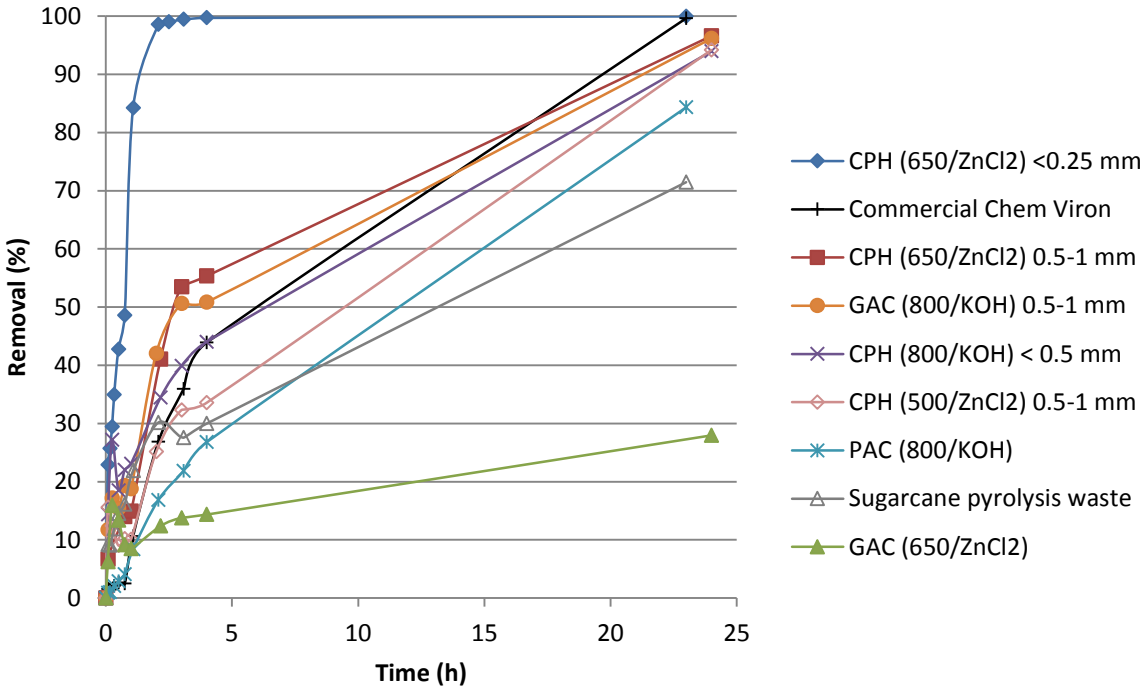

Figure 10 Methylene Blue adsorption experiments, c_0 (MB)=50 mg/l, m(ads.) = 1 g/l.

In As removal tests the adsorbent provided by Kemira and all the agrowaste originated activated carbons were more efficient than commercial adsorbent ChemViron. Figure 11 shows that the adsorption was very rapid already in the beginning of the experiment and for the three best adsorbents, Kemira adsorbent, MSIP and Corn Cop, the removal efficiency reached almost 100% during the first two hours.

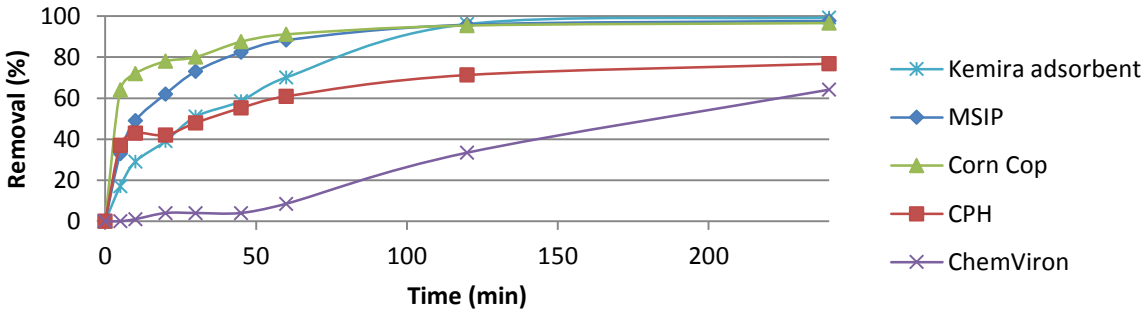

Figure 11 As removal in batch experiments.

In fixed-bed column experiments the highest removal efficiency was found with Sachtofer. The ash granules did not have mechanical strength for the long experiment and the results were dropped out from Figure 12. The breakthrough point in the Sachtofer and activated carbon curves were not

achieved, because the feeding solution flow rate was kept very low to avoid the enormous amount of wastewater. However, the removal efficiencies are pretty good for all the tested impurities.

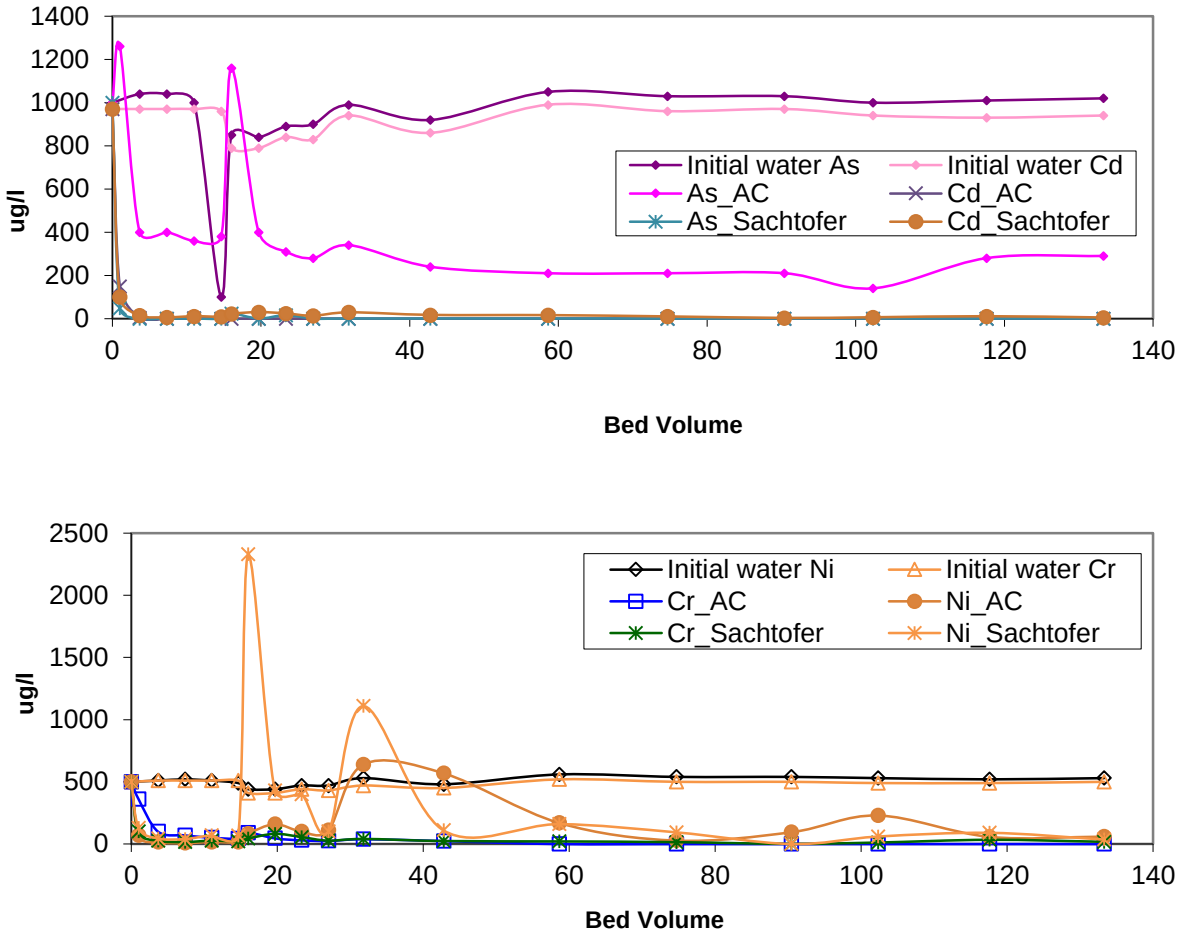

Figure 12 Effluent As and Ni concentrations as a function of bed volumes.

Photocatalysis results

The experimental results from both the reactors (quartz and Teflon) are compared in Table 5. The aim of this comparison was to find out the effect of the reactor configuration on the degradation of the studied compounds. The experimental results were fitted to the pseudo-first order kinetics, ad based on the apparent first order rate constant reaction half-lives ($t_{1/2}$) and the specific applied energy values (E_{SAE}) were calculated. This is especially important for the calculation of the values of the applied energy. According to Bolton et al. (2001), the advanced oxidation process should not affect the calculation of the proposed figures of merit. (Pirilä et al. 2015)

Table 5 Comparison of the reactor configuration with the initial pollutant concentration of 15 mg/l and the catalyst dose of 200 mg/l in alkaline conditions in distilled water solutions (Pirilä et al. 2015).

Pollutant	Quartz reactor				Teflon reactor			
	Initial pH	Rem.(%) 45 min	$t_{1/2}$ (min)	E_{SAE} (kWhmol^{-1})	Initial pH	Rem.(%) 45 min	$t_{1/2}$ (min)	E_{SAE} (kWhmol^{-1})
BPA	9	62	40	1337	10	59	19	326
PCOU	8	36	86	799	10	99	15	179
PHA	8	43	48	1169	10	94	9	98
Diuron	9.6	68	26	560	10	98	7	123

Table 5 shows the initial pH, the pollutant removal after 45 minutes of photocatalysis, the calculated reaction half-lives and the estimated specific applied energies obtained from the experiments done in distilled water solutions in both the reactor types. Based on the results it is obvious that the Teflon reactor is more efficient in the removal of the pollutants, when all the parameters in Table 22 are considered. This might be due to the fact that the Teflon reactor is annular meaning that the lamp is closer to the irradiated solution giving a higher irradiance power than that in the quartz reactor. In addition, in the Teflon reactor the suspension with the pollutant and the catalyst is irradiated continuously, as with the quartz reactor the suspension is circulated outside the reactor, thus reducing the effective irradiance time. Also the smaller total volume of the suspended solutions might have an effect, since in the Teflon reactor the total volume is only half of that of the quartz reactor. The initial pH values were not exactly the same in both the reactors which also might have affected the different purification results. The E_{SAE} values are from 4- to 10-fold higher in the quartz reactor than in the Teflon reactor. The quartz reactor has six lamps, i.e. 6x15 W, compared to the Teflon reactor which has only one lamp of 36 W, which means that the Teflon reactor has lower energy consumption due to the lamp power needed. (Pirilä et al. 2015)

Fig. 13 shows that the industrial wastewater matrix, even though diluted, remarkably affects the purification efficiency of the model pollutants. However, all the studied compounds reached over 70% removal percentages in the wastewater matrix where as in distilled water the final removal levels were over 90% in all the cases. There are several other organic compounds present in the wastewater, and they are most likely competing for the active sites on the catalyst surface, and thus decrease the removal of the studied compounds. (Pirilä et al. 2015)

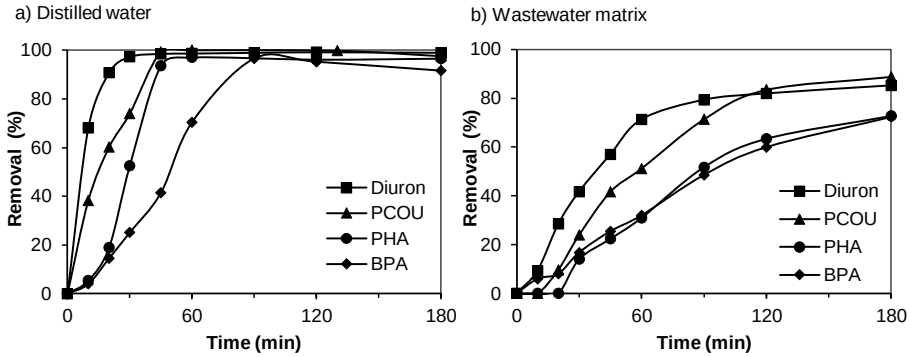

Figure 13 Comparison of the photocatalytic removal of the model pollutants in a) distilled water and in b) the wastewater matrix. The initial pollutant concentration of 15 mg/l and catalyst dose of 200 mg/l in alkaline conditions (Pirilä et al. 2015).

The degradation of the organic compounds was studied by analysing the total organic compounds (TOC) from the water samples. The TOC removal values in 3 hours in the photocatalytic experiments both in distilled water and in industrial wastewater solutions are shown in Fig. 14. The diluted wastewater without the added model pollutants was also studied for the TOC removal for

comparison. The TOC removals in distilled water solutions are evidently higher than in wastewater, most probably due to the lower initial TOC values, i.e. the diluted wastewater solution had approximately a 10 times higher TOC content in the beginning. The maximum TOC removal was observed in the case of BPA degradation (~70%). (Pirilä et al. 2015)

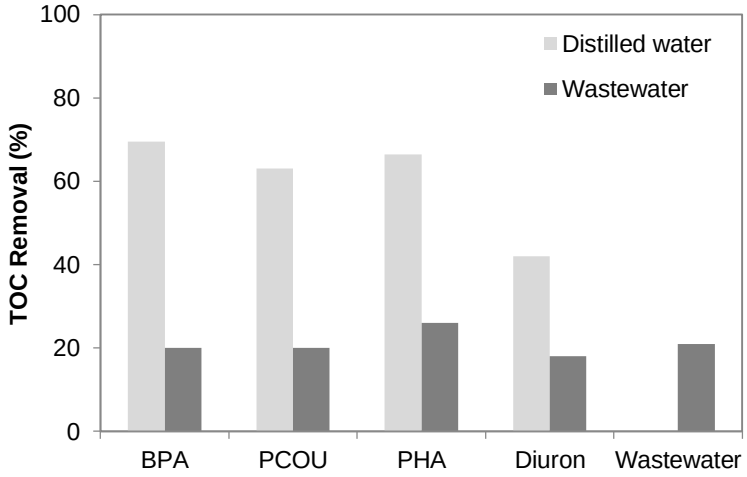

Figure 14 Total organic carbon removal after 3 hours of UV-A irradiation with the initial pollutant concentrations of 15 mg/l and a catalyst dose of 200 mg/l both in distilled water solutions and in diluted wastewater. The last column represents the TOC removal from the diluted wastewater solution without added model pollutants (Pirilä et al. 2015).

Nitrogen compounds

Oxidation of nitrogen compounds (nitrate, nitrite and ammonium) was studied from the real mine wastewater. Two photocatalysts (Aeroxide P25 and Hombitan S141) were used in the experiments. The highest removal was observed for nitrite while the nitrate concentration was increased during the experiments. Also concentration of ammonium increased a little during the experiments.

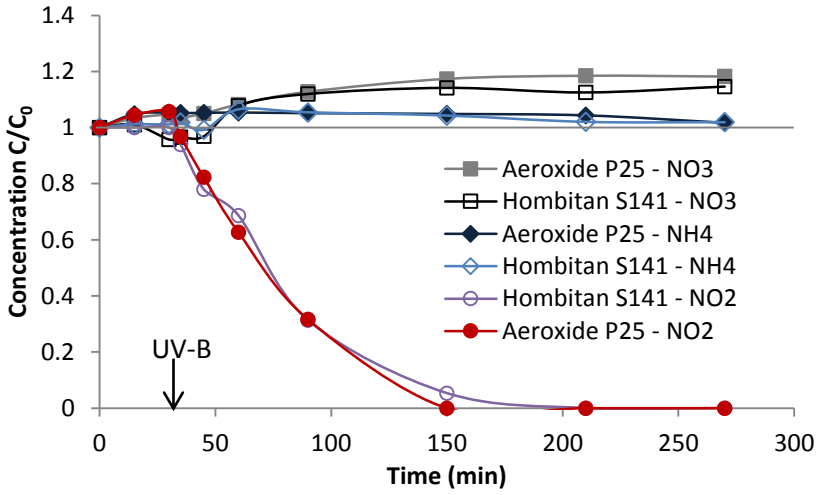

Figure 15 Oxidation of nitrogen compounds in the real mine wastewater.

Hybrid membrane results

Bisphenol-A removal from synthetic wastewater was studied with the photocatalytic membrane reactor. In Fig. 16 is represented the BPA rejections during filtration experiments. The UV-A lamps were turned on after 40 minutes of experiment. As can be seen from the figure, NF90 had the highest BPA removal while coated NF90 gave a smaller rejection efficiency. The NF270 membranes had lower rejections compared to all the NF90 membranes. As a summary from the experiments, membrane coating did not clearly improve the rejection coefficient of BPA.

After turning the UV-light on, membrane characteristics changed and therefore the rejection of BPA decreased with the coated membranes, however, the rejection was slightly increased with the commercial membranes. Also the permeate flux decreased and increased with the commercial and coated nanofiltration membranes, respectively, after turning the lights on.

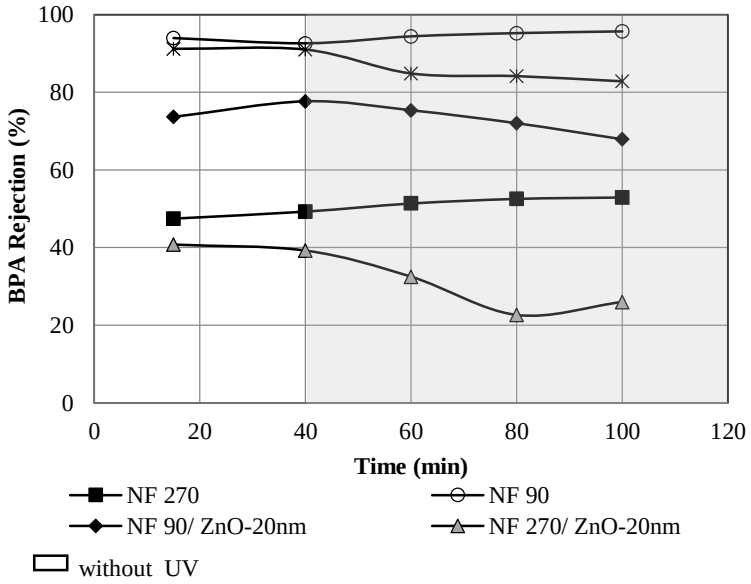

Figure 16 Rejection of BPA with the commercial and coated membranes during the filtration experiments.

UV-A light affected on the permeate flux values (Figure 17). The permeate flux of commercial membranes decreased after the lights were turned on while the rejection coefficient values were slightly increased (Figure 16). The permeate flux of the coated membranes was, however, increased during the exposition to the UV-A light. The permeate flux increase was observed due to the membrane coating wearing which was intensified in the presence of UV-light. Visual changes on the membrane surface were noticed after photocatalytic experiments. The membrane surface became yellowish in the areas which were exposed to the UV-light and also the coating was noticeably depleted.

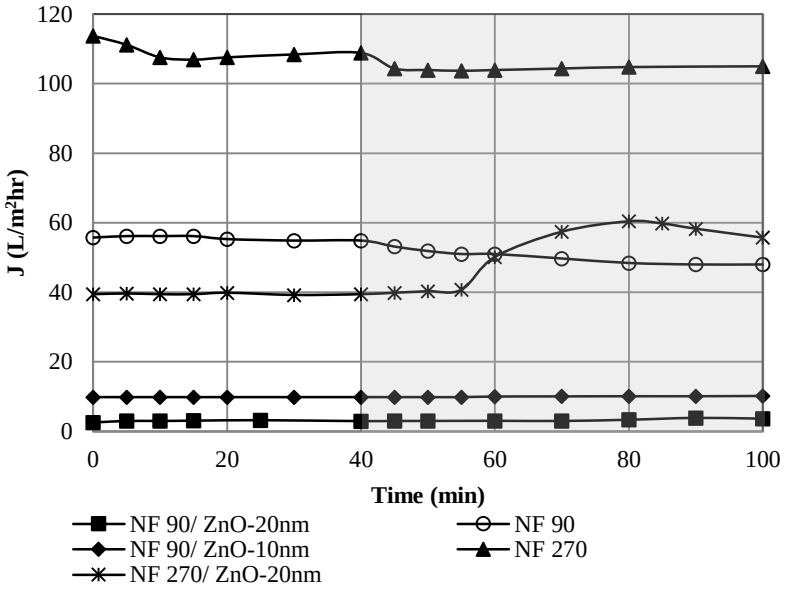

Figure 17 Permeate flux of commercial and coated nanofiltration membranes.

Hybrid adsorption material development

The TiO_2 coated Sachtofer PR granules were characterized by several different methods, such as Scanning electron microscope imaging and elemental mapping (SEM JEOL SM-6490LV equipped with Oxford INCA x-sight EDS-detector). Figure 18 shows the SEM images taken from the original Sachtofer PR and three different coated samples.

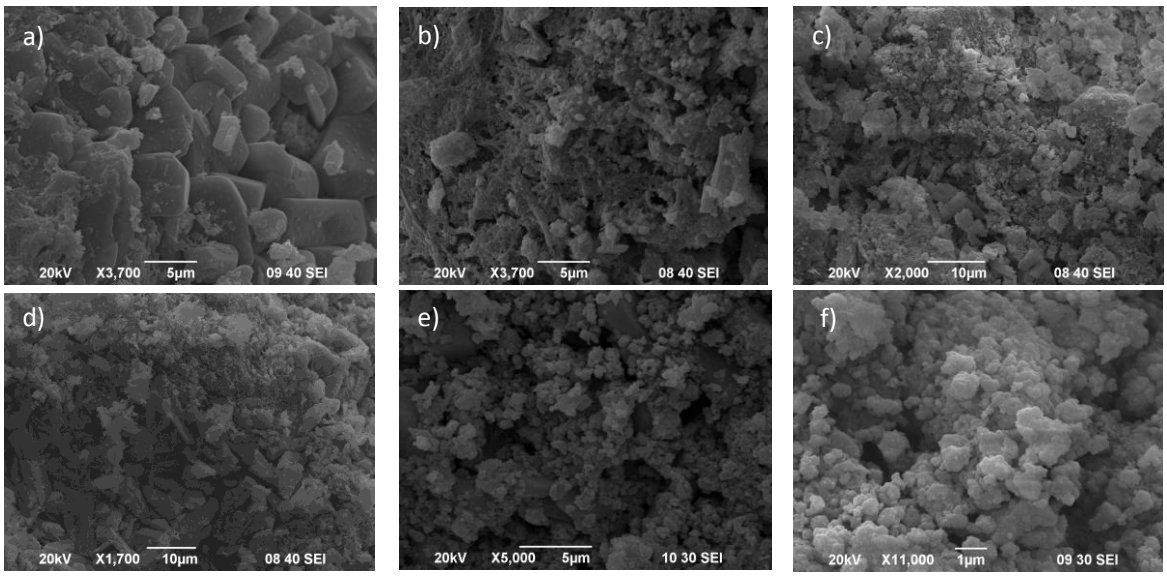

Figure 18. SEM micrographs from a) original Sachtofer PR, and with b) 5 dip-coating layers with 0.1 M TiO_2 precursor, c) and d) 1 dip-coating layer with 0.5 M TiO_2 precursor, e) and f) 1 dip-coating layer with a 10 w-% suspension of Hombicat UV100 TiO_2.

The original Sachtofer PR granules in Fig. 18 show quite big crystals mainly of gypsum and calcite detected by XRD. There clearly are TiO_2 layers visible after all the coatings shown in Fig. 18 b-f. However, Fig. 18 c and d show that only one coating layer with the 0.5 M TiO_2 precursor is not enough to get a total coverage and the coating layer is uneven and in some parts the surface of the original crystals of Sachtofer PR is still visible. With 5 dip-coatings in the 0.1 M TiO_2 precursor the

original surface has totally been covered. The coating done with the commercial TiO_2 slurry, shown in Fig. 18 e and f, shows the typical TiO_2 particles on the surface. In Fig. 18 e the original Sachtofer PR surface is still visible, and thus the coating layer is not fully covering the surface.

The coated materials were studied for their ability to remove the organic model compound methylene blue from water both by photocatalysis and adsorption. However, these results are not encouraging and therefore are not included into this report. The coating process should have been optimized in order to get a more active TiO_2 layer, e.g. the coating layers, the precursor concentrations, the calcination temperature and time should have been optimized in order not to block the existing pores on the Sachtofer material. However, it would be interesting to continue this research later in the future.

Sustainability analysis

Qualitative method

The sustainability assessment questionnaire contained 54 questions. In this questionnaire, scores of -1 or 1 were allocated to each question based on the assumption that a water treatment process either has a positive or a negative effect on the environment, the economy and the people. To make the comparison more concrete, the results were visualized as spider diagrams (Fig. 19). The larger the diagram area is, the better the process follows the sustainability assessment criteria.

The qualitative sustainability assessment shows that the AA-Reg has the highest environmental impact mostly because of producing waste and using extra chemicals. Fe-GAC has the highest cost of the used adsorbents, but since renewable and secondary materials could be used as the adsorbent the amount of waste could be less and the materials use could be more oprimal. From the social point of view AA-Reg has both positive and negative impacts. Negative is that the use of chemicals has health and safety risks for employees working in the process, but also positive as an advanced training related to the health and safety issues on the used chemicals/raw materials is most probably needed. (Saavalainen et al. 2013)

Figure 19 Qualitative sustainability assessment results (Saavalainen et al. 2013).

Quantitative method

The resources used for the process are converted to natural resource sustainability (NRS) (Table 6) values and environmental burdens sustainability (EBS) values using the Gabi LCA v4.3 software. The Dimensionless Normalized Environmental Burdens Sustainability (DNEBS) values: from all steps Cradle to Grave are shown in Table 7.

Table 6 Natural Resources Sustainability Values (Saavalainen et al. 2013).

	Units	AA	Fe-GAC	AA-Reg	DW
Cradle to Gate					
Energy	MJ / m^3	2.24	4.46	10.09	6.27
Materials	kg / m^3	0.18	6.63	0.65	0.69
Water	m^3 / m^3	0.00	0.06	0.06	1.14
Gate to Gate					
Energy	MJ / m^3			0.44	1.4
Materials	kg / m^3	0.12	1.03	0.59	0.02
Water	m^3 / m^3			0.008	0.18

Table 7 Dimensionless Normalized Environmental Burdens Sustainability (DNEBS) values (Cradle to Grave (Saavalainen et al. 2013).

	AA	Fe-GAC	AA-Reg	DW
Cradle to Grave				
Air	0.09	4.97	0.579	0.186
Water	3.47	3.13	4.44	1.57
Land	82.1	710	18.2	0.00288
Cradle to Gate				
Air	0.0902	4.97	0.579	0.186
Water	3.47	3.13	3.94	1.57
Land	-	-	-	-
Gate to Gate				
Air	-	-	-	-
Water	-	-	0.497	-
Land	82.1	710	18.2	0.00288
Total	**86**	**718**	**23**	**2**

The NRS and EBS will increase notably by the introduction of an adsorption step for arsenic removal in a drinking water plant. The AA has the lowest NRS and regeneration (AA-Reg) will lead to the lowest EBS. The land index in EBS is the highest for all the tested adsorbents. The adsorption capacity is the main impacting parameter from the environmental perspective. (Saavalainen et al. 2013)

Outcomes of the project

Scientific journal articles

Pirilä M, Saouabe M, Ojala S, Drault F, Valtanen A, Huuhtanen M, Brahmi R & Keiski RL. Photocatalytic degradation of organic pollutants in wastewater. Submitted to Topics in Catalysis 6/2014, in collaboration with AOPI –project (AF). Replied to review -comments 4/2015.

Cruz GJF., Matějová L, Pirilä M, Ainassaari K, Solis JL, Cruz JF, Šolcová O & Keiski RL. A comparative study on activated carbons derived from a broad range of agro-industrial wastes in removal of large molecular size organic pollutants in aqueous-phase. Submitted to Water Air and Soil Pollution 12/2014, in collaboration with AdMatU –project (AF). Replied to review -comments 4/2015.

Cruz GJF, Pirilä M, Matějová L, Ainassaari K, Solis JL, Fajgar R, Šolcová O & Keiski RL. ZnCl2-based-activated carbon produced from two novel precursors as promising material for application in the treatment of polluted water. Submitted to Journal of Environmental Management 1/2015, in collaboration with AdMatU –project (AF).

Chavan KR, Saavalainen P, Marathe KV, Keiski RL & Yadav GD. Lifecycle assessment of technologies for removal of arsenic from water. Submitted to ACS Sustainable Chemistry and Engineering 3/2015.

Pirilä M, Cruz GJF, Ainassaari K, Gomez MM, Matějová L & Keiski RL. Removal of As(V), Cd(II) and Pb(II) from multicomponent aqueous systems using activated carbons. Submitted to Water Air and Soil Pollution 4/2015.

Häyrynen P, Landaburu-Aguirre J, Isomäki R, Kääriäinen ML & Keiski RL. Sulphate removal from mine wastewaters by nanofiltration. Manuscript will be submitted to Separation and Purification Technology Journal in Spring 2015, in collaboration with Sulka-project.

García V, Häyrynen P, Landaburu-Aguirre J, Pirilä M, Keiski RL & Urtiaga A (2014) Purification techniques for the recovery of valuable compounds from acid mine drainage and cyanide tailings: application of green engineering principles. J Chem Technol Biotechnol 89: 803–813.

Häyrynen P, Galambos ?, Szekrnyes K Keiski RL & Vatai V. (2013) Concentration of nitrogen compounds and heavy metais by a reverse osmosis - membrane distillation hybrid process. Julkaistu Permea 2013 Conference proceedings -julkaisussa.

Pirilä M, Lenkkeri R, Goldmann WM, Kordás K & Keiski RL. (2013). Photocatalytic degradation of butanol in aqueous solutions by TiO2 nanofibers. Topics in Catalysis 56 (9-10), 630-636.

Piia Häyrynen, Junkal Landaburu-Aguirre, Eva Pongrácz & Riitta L. Keiski (2012) Study of permeate flux in micellar-enhanced ultrafiltration on a semi-pilot scale: Simultaneous removal of heavy metals from phosphorous rich real wastewaters. Separation and Purification Technology 93, 59-66.

Cruz G, Pirilä M, Huuhtanen M, Carrión L, Alvarenga E & Keiski RL. 2011. Production of Activated Carbon from Cocoa (Theobroma cacao) Pod Husk. 2012. J Civil Environment Eng 2:109. doi: 10.4172/2165-784X.1000109.

Gadipelly C, Pirilä M, Shafqat K, Rathod VK, Marathe KV, Valtanen A, Huuhtanen M, Yadav GD & Keiski RL. Photocatalytic degradation of amoxicillin in aqueous streams. Manuscript.

Jadhav S, Häyrynen P, Marathe KV, Rathod VK, Keiski RL & Yadav G. Experimental and theoretical analysis of nanofiltration membranes for treatment of sulfate and arsenic laden wastewaters from mining industries. Manuscript.

Pirilä M, Lenkkeri R, Martikainen M, Saouabe M, Brahmi R, Huuhtanen M, Pekonen P & Keiski RL. Photocatalytic decolorization of synthetic dye wastewater by titanium dioxide based materials. Manuscript.

Scientific conference presentations

NaMiBiTech conference, Akhawayn University Ifrane, Morocco, 26-28.11.2014. Oral presentation "Low temperature steam reforming of ethanol over CNT-based catalysts" / Prem K. Seelam.

No-Waste project: Marie Curie Actions FP7 workshop, Chouaib Doukkali University, El Jadida, Morocco, 23-24.11.2014. Oral presentations: "Research Ethics" / Riitta Keiski, "Sustainability assessment analysis" / Riitta Keiski, "Adsorbents in water treatment" / Kaisu Ainassaari, "In situ FT-IR spectroscopic studies on CO_2/CH_4 adsorption and reaction studies"/ Prem K. Seelam.

16th Nordic Symposium on Catalysis, Oslo, Norway, 15.-17.6.2014. Poster presentation and abstract "Photocatalytic degradation of organic pollutants in wastewater" (Minna Pirilä, Mika Huuhtanen) in collaboration with AOPI-project.

IX Ibero-American Congress on Membrane Science and Technology, Spain, 25.-28.5.2014. Poster presentation and abstract "Modified NF270 membrane in sulphate removal" (Riitta Keiski, Piia Häyrynen), in collaboration with Sulka-project (EAKR).

IX Ibero-American Congress on Membrane Science and Technology, Spain, 25.-28.5.2014. Keynote-speech and abstract "Current Industrial Wastewater Problems and Treatment Methods in Finland – The Focus Areas in Research" (R.L. Keiski), in collaboration with AOPI-, AdMatU- and SULKA-projects.

HYMEPRO –project presentation in GREENTECH - The application of Green Technologies for sustainable water purification and re-use –meeting in Santader, University of Cantabria, Spain 27.2. – 1.3.2013. Oral presentation by Piia Häyrynen, Paula Saavalainen and Minna Pirilä.

HYMEPRO –project presentation in EU ERA-MIN Roadmapping conference in Lisbon, Portugal 11 .- 1 3.3.2013. Poster presentation / Minna Pirilä.

4th International Conference on Semiconductor Photochemistry (SP4), Prague, Czech Republic, 23-27.6.2013. Abstract (SP4 Book of Abstracts), oral presentation and poster presentation / Minna Pirilä.

Water research at the University of Oulu -conference, 15.8.2013. 2 oral presentations + 4 poster presentations + abstracts to the book "Proceedings of the WaRes conference" / Minna Pirilä, Piia Häyrynen, Paula Saavalainen, Junkal Landaburu.

Permea 2013, Warsaw, Poland, 15.-19.9.2013 Oral presentation and conference paper / Piia Häyrynen.

Clean Air Research at University of Oulu –2nd SkyPro conference 12.11.2013. Poster presentation / Minna Pirilä.

New vistas in water treatment technologies –Workshop, Institute of Chemical Technology, Mumbai, India, 26.11.2013. Plenary lecture "Water Treatment Challenges" / Minna Pirilä.

15th Nordic Symposium on Catalysis –conference, Mariehamn 10.-1 2.6.2012. Two poster presentations and abstracts / Minna Pirilä, Ritva Lenkkeri, Riitta Keiski.

EUROMEMBRANE 2012 -conference, London 23.-27.9.2012, poster presentation and abstract / Piia Häyrynen.

EU INDIA STI COOPERATION DAYS, NGRI, HYDERABAD, INDIA, 8.-9.11.2012. 2 poster presentations. In collaboration with NEW-INDIGO Greentech –project.

26.-27.11.2012 Tekes final seminar on water program: BioRefine and Water –Paving the Way for Bioeconomy. Poster of Hymepro-project / Minna Pirilä.

International conference on Sustainable Mineral Processing, SUSMP'12 University of Oulu, 10-13 December 2012. Oral presentation and abstract / Minna Pirilä, Paula Saavalainen, Riitta Keiski.

MoniMineWater –project final seminar "Environmental measurements and their future demands." 27.9.2011. Poster presentation / Minna Pirilä, Piia Häyrynen, Junkal Landaburu, Ritva Lenkkeri.

Academic theses

Doctoral Theses

Junkal Landaburu-Aguirre: Micellar enhanced ultrafiltration for the removal of heavy metals from phosphorous-rich wastewaters. From end-of-pipe to clean technology (2012)

Minna Pirilä: Adsorption and photocatalysis in water treatment – Abundant, active, inexpensive materials and methods (2015)

Master's theses

Cecilia Castro: Preparation of activated carbons from biomass and their use in adsorption of arsenic (2012)

Anastasia Dubatova: Removal of nitrogen compounds from industrial waters by photocatalysis and adsorption (2013)

Khawer Shafqat: Use of photocatalysis for the removal of pesticides from water (2013)

Buddhika Rathanayeke: The removal of organic pollutants from wastewater by photocatalytic degradation compared to hybrid photocatalytic membrane technique (2014-2015)

Bachelor's theses

Aki Koskela: Sulfaattien poisto ja konsentrointi vesiliuoksesta nanosuodatuksella (2015)

Ada Laitinen: Quality, legislation and treatment of natural waters and municipal waste waters in Finland (2012)

Janne Vähämäki: Utilization of the dry distillation products of wood (2012)

Veikko Pekkala: Wastewaters and their treatment in the Finnish mining industry (2013)

Reports

"Degradation of Organic Pollutants by Photocatalysis, Photolysis and Adsorption" (Buddhika Rathnayake). Advanced Practical Training Report.

"Adsorption and photocatalysis for removal of methylene blue from water" (Anastasia Dubatova). Research methodology course training report.

"Advanced oxidation processes in industrial wastewater treatment. Degradation of organic pollutants by photocatalysis and photolysis on TiO_2 with UV-A" (Fabien Drault). Student exchange internship report.

"Application of adsorption and photocatalysis for both synthetic and real wastewater treatment" (Khawer Shafqat) Advanced practical training report.

"Photocatalytic performance of titanium oxide-based catalysts in n-butanol decomposition" (Werner Marcelo Goldmann) Advanced practical training report.

"Activated carbon production from cocoa pod husk and its use in adsorption of arsenic from aqueous solutions" (Emilio Alvarenga) Advanced practical training report.

"Removal of sulphate by nanofiltration" Doriane Chrysanthos. Research exchange report.

"Synthesis of sulfated starch and filtration of wastewater" Louis Maresse. Research exchange report.

"Hybrid material development by adding a layer of semiconductor TiO_2 onto the surface of industrial side product granules (Sachtofer PR)". (Minna Pirilä) Research exchange report.

"Kaivosteollisuuden ympäristöongelmat ja niiden hallinta" (Riitta L. Keiski) Artikkeli Luonnon Tutkija 1/2013.

"Puhtaan veden perässä" (Riitta L. Keiski) Lehtihaastattelu Aktuumi (Riitta L. Keiski) 9/2013.

Relevance of the research

The purification of wastewater will reduce the harm towards the environment by eliminating nutrient and heavy metal discharges, improve the resource efficiency of valuable compounds and promote water re-use and reduce freshwater consumption. The conduction of this research helps industry to employ an eco-efficient and innovative hybrid process that removes water pollutants from effluents with high efficiency. Further, this study reinforces the co-operation between companies by converting wastes and side products from one enterprise into a valuable and recyclable raw material for another enterprise. Therefore, the recovery and reuse of such valuable compounds as well as the removal of pollutants from wastewaters improves the sustainability of many industrial processes.

Companies that design water treatment facilities benefit from the results of this project by improving their competitiveness at national and international level due to the developed hybrid water treatment technology. Disadvantages of these process when used alone can be overcome and in that way sustainability and process efficiency can be improved. For example, one of the biggest challenges in membrane technology is membrane fouling which can be prevented by the development of self-cleaning membranes. Further, there is a high marketing potential due to the possibility to extend the markets to drinking water treatment.

To conclude, within the HYMEPRO –project the hybrid method development was achieved. However, the method needs further research and studies in order to scale it up and to use it in industrial applications. For example, the mechanical strength of the coated membranes needs more development, and the utilization of solar light would give the method more relevance later in the future.

References

Chavan KR, Saavalainen P, Marathe KV, Keiski RL & Yadav GD (2015) Lifecycle assessment of technologies for removal of arsenic from water. Submitted to ACS Sustainable Chemistry and Engineering 3/2015.

Cruz G, Pirilä M, Huuhtanen M, Carrión L, Alvarenga E & Keiski RL (2011) Production of activated carbon from cocoa (Theobroma cacao) pod husk. 2012. J Civil Environment Eng. 2:109. doi: 10.4172/2165-784X.1000109.

Gupta VK & Ali I (2013) Environmental Water. Advances in Treatment, Remediation and Recycling. Oxford, Elsevier. 1st ed.

Leong S, Razmjou A, Wang K, Hapgood K, Zhang X & Wang H (2014) TiO_2 based photocatalytic membranes: A review. J. Membr. Sci. 12/15;472(0):167–184.

Mavrov V, Erwe T, Blocher C & Chmiel H (2003) Study of new integrated process combining adsorption, membrane separation and flotation for heavy metal removal from wastewater. Desalination 157 97–104.

Pirilä M, Saouabe M, Ojala S, Drault F, Valtanen A, Huuhtanen M, Brahmi R & Keiski RL (2015) Photocatalytic degradation of organic pollutants in wastewater. Submitted to Topics in Catalysis 6/2014, in collaboration with AOPI –project (AF). Replied to review -comments 4/2015.

Saavalainen P, Chavan K, Pirilä M, Häyrynen P, Dominguez –Ramos A, Marathe KV, Yadav GD, Irabien A, Pongrácz E & Keiski RL (2013) Sustainability assessment of arsenic removal from natural waters by adsorption. Poster presentation in Wares –conference (Water research at the University of Oulu –conference) 15.8.2013.

Van der Bruggen B, Mänttäri M & Nyström M (2008) Drawbacks of applying nanofiltration and how to avoid them: A review. Sep. and Purif. Technology 10/22;63(2):251–263.

5 LAPPEENRANTA UNIVERSITY OF TECHNOLOGY (LUT)

Laboratory of Green Chemistry (LGC)

Irina Levchuk Researcher, Eveliina Repo Senior Researcher and Mika Sillanpää Supervisor

Lappeenranta University of Technology, Laboratory of Green Chemistry, Sammonkatu 12 50130, Mikkeli, Finland

ASTRaI

David Cameron, Marja-Leena Kääriäinen

(ASTRaL was merged to the Laboratory of Green Chemistry during the project. Cameron and Kääriäinen are not working at LUT for the moment.)

Membrane research group

Mika Mänttäri Author, Supervisor

Mari Kallioinen Supervisor

Arto Pihlajamäki Supervisor

Daria Nevstrueva Researcher, Juuso Huittinen MSc student, Mikko Brotell MSc. Student and Helvi Turkia Laboratory technician

Lappeenranta University of Technology, Membrane research group, Skinarilankatu 34, 53850, Lappeenranta, Finland

Abstract

The role of the Laboratory of Green Chemistry (LGC) within this project was preparation of catalytic membranes operating in the visible light region, testing the performance of membranes in visible light (using LEDs), determination of the stability and the efficiency of degradation of organic pollutants, cooperation with other research groups regarding material characterization, testing and selection of water to be purified. LUT ASTRaL focused on the development of ALD (atomic layer deposition) methods to modify polymeric membranes. The modified membranes were tested by the LUT membrane research group and the University of Oulu. The LUT membrane research group developed also a hybrid process concept to purify nutrient rich waste streams and to the recovery nitrogen as a concentrated by-product.

Objectives of the research

The research carried out by LUT was made in three research groups: ASTRaL, Green Chemistry (LCG) and Membrane Technology. The main objective of the work made by ASTRal was to develop atomic layer deposition (ALD) methods to modify membrane properties. The main objectives of research conducted by the LGC group within the HYMEPRO project were preparation, characterization and testing of photocatalytically active TiO_2 thin films doped with gold and silver nanoparticles. The membrane research group focused on the testing and development of the ALD coatings together with ASTRaL. In addition, the aim was to develop a purification process for nutrient rich wastewater.

Materials and methods

Material synthesis

Synthesis of TiO_2/SiO_2 thin films doped with gold nanospheres

Firstly, silica sol was prepared by hydrolyzing MTEOS at pH 3.5. Detailed procedure can be found elsewhere [1]. Sol of titanium dioxide doped with gold nanoparticles was prepared by addition of the $HAuCl_4$ solution to TiO_2 nanoparticles (Degussa P25) suspended in Milli-Q water so that Au/TiO_2 ratios (wt.%) were 0, 0.05, 0.5, 1.25 and 5%. Gold was reduced by freshly prepared 0.1M $NaBH_4$ under vigorous stirring. In the reference sample (Au/TiO_2 ratio 0), the volume of added $NaBH_4$ was equal to that in a sample with the ratio of 1.25%. After that, pH of the solution was adjusted to 10 using 1M NaOH. The obtained suspensions were stirred (650 rpm) in darkness for 3 h. Then suspensions were centrifuged for 35 min at 10 000 rpm and 14°C in order to get rid of the supernatant, washed a few times with Milli-Q water and centrifuged again. The obtained TiO_2/Au pastes were added to hybrid silica sol. Coatings were prepared on Si wafers (3 x 3 cm) using a dip coating method (speed - 50 mm min^{-1} and dip duration - 10 sec). After deposition, thin films were dried in the oven at 120°C for 20h.

Synthesis of TiO_2/SiO_2 thin films doped with gold bipyramid-like nanoparticles

Silica sol was prepared as described above. Sol of gold bipyramid-like nanoparticles (Au BP) was synthesized according to the procedure reported in [2]. Hybrid TiO_2/Au pastes were prepared by dispersion of commercially available TiO_2 (Degussa P25) in water, addition of a calculated volume of Au BP sol followed by sonication and the supernatant discard. The obtained pastes were added to the silica sol and sonicated. Coatings were prepared on Si wafers (3 x 3 cm) using a dip coating method (speed - 50 mm min^{-1} and dip duration - 10 sec). After deposition, thin films were dried in the oven at 120°C for 20h.

Material characterization

For the estimation of size and shape of gold nanoparticles, TEM images were done using a TOPCON EM002B transmission electron microscope operating at 200 kV. The sample preparation for TEM analysis consisted of scrapping of prepared thin films and direct deposition of fragments onto a microscopy copper grid coated with a holey carbon film.

Morphology and thickness of the prepared thin films were studied using a scanning electron microscope ZEISS LEO 1550 and Form Talysurf Series 2 PGI, respectively. Porosity of some of the prepared thin films was measured by the means of SOPRA Ellipsometer EP5 (Semilab) equipped with a CCD array detector (190 nm – 870 nm). UV-visible measurements were done using a PerkinElmer Lambda 750 UV/VIS/NIR spectrometer. X-ray photoelectron spectrometer Thermo Fisher Scientific ESCALAB 250Xi was used in order to confirm the presence of Au in the coatings.

The diffused reflectance measurements were used for the evaluation of the band gap of synthesized samples. The fiber UV-Vis spectrometer AvaSpec-2048 (Avantes) equipped with AvaLight-DHS deuterium (UV) and halogen lamps (Vis region) was utilized in this study. The optical path was built in such a way that one optical fiber was connected to the lamps providing illumination and another – to the spectrometer for recording the signal. The band gap calculations were done based on the obtained reflectance measurements (from 250 nm – 400 nm). Barium sulfate was used as a reference.

The measurements of contact angle were performed in order to evaluate the wettability of synthesized thin films before and after the UVC pretreatment. Measurements were conducted at room temperature (22±2°C) with a GBX Digidrop Goniometer connected with digital camera. Milli-Q water droplets with the volume of 10 μL were deposited on different locations of the sample surfaces and contact angles were recorded immediately. The mean values of contact angle were calculated using the WinDrop++ software from five measurements per sample.

The loading of TiO_2 was determined with an "Activa" Jobin Yvon inductively coupled plasma optical emission spectrometer (ICP-OES). The sample preparation consisted of dissolving of TiO_2/SiO_2 and TiO_2/SiO_2-Au NP coatings in a mixture of H_2SO_4, HNO_3 and HF at 120°C.

Photocatalytic tests

Model solution containing formic acid with the concentration of 50 ppm was used in order to estimate and compare photocatalytic activity of synthesized materials. High Performance Liquid Chromatograph (HPLC) VARIAN ProStar equipped with column COREGEL-87H3 (300 × 7.8 mm) and UV-Vis detector (λ = 210 nm) was used for the measurements of formic acid concentration. Sulfuric acid (C = 5 × 10^{-3} mol L^{-1}) was utilized as a mobile phase with the flow rate of 0.7 mL min^{-1}.

Photocatalytic tests were conducted at room temperature (22 ± 2°C) in a 100 cm^3 batch cylindrical reactor wrapped inside an aluminum foil. The diameter of the Pyrex optical window of the reactor was 4 cm. Thin films deposited on a silicon wafer with dimensions of 3 cm × 3 cm were located in the reactor and covered by 3 cm × 3 cm glass substrate preventing floating of the sample. A magnetic stirrer (RCT basic IKAMAG®) was used for mixing 30 mL solution with the speed of about 600 rpm. Sampling was carried out after each 30 min, the volume of the sample was 0.3 mL and changes in FA concentration were monitored with HPLC. The first 30 min of each photocatalytic experiment was performed in darkness in order to reach the adsorption-desorption equilibrium. It should be noticed that each experiment was repeated at least three times.

A high pressure mercury lamp (Philips HPK 125 W) was used as a source of irradiation in all experiments conducted in the UV-Vis region. Before starting the experiments the lamp was stabilized for at least 30 min. Owing to the circulation water cell with Pyrex filters, no infrared and UVC beams reach the reactor. Experiments in Visible light only were performed using a LED lamp. Before and after each experiment, the radiant flux measurements were done with a VLX-3W radiometer using CX-365 (UVA) and CX-312 (UVB) detectors.

2.2 Testing of ALD coated membranes

ALD coatings were mostly made on the surface of polymeric 20 kDa polyethersulphone UF membrane. Deposition temperature was aimed to be high in order to get some crystalline ZnO. In addition two various oxidizing precursors were used; water and ammonium hydroxide. In our earlier work (M.-L. Kääriäinen et al.) it has been found that N-doping increased the conductivity of TiO_2. Therefore NH_4OH was used to receive a nitrogen doping effect which could change electrical properties of the membrane. A certain type of electrical charge can affect especially the retention characteristics of a membrane in filtration. Zinc oxide thickness was aimed to be 30 nm. The tests were: T=93°C, ZnO-N; T=86°C, ZnO-N; T=86°C, ZnO.

ALD coated membranes and virgin membranes were characterised by measuring the membrane permeabilities and retention of neutral (polyethyleglycols having diffrent molar mass, 200 ppm solution) and ionic compounds (magnesium sulphate, 200 ppm solution). Dead-end stirred cell (Amicon, 40 cm^2 membrane area) and cross-flow cell (10 cm^2 membrane area) filters were used in the filtration experiments when ALD coated membranes were tested. Experiments were made as a function of pressure. Fouling of membranes was evaluated by filtering the effluents from Honkajoki Oy and by measuring the difference in pure water fluxes before and after the effluent filtration.

Filtration and evaporation experiments with condensate (Honkajoki effluent)

Honkajoki Oy treats animal-based raw materials. The condensate solution from the drying stage contains 800-4500 mg/L nitrogen, mostly ammonium nitrogen. The nitrogen content of the condensate is too high to be discharged. In addition, the condensate contained a significant amount of organic acids. The tested condensate contained 850 mg/L (1st sample) and 2500 mg/L (2nd sample) of NH_4^+-nitrogen. The first sample (pH 9.2) was used in membrane screening experiments and the second sample (pH 9.3) in larger scale experiments.

Purification of the condensate was studied using the DSS LabStak M20 cross-flow filter. Ten different NF and RO membranes were tested first at different pressures to evaluate their fluxes and retentions for ammonium ions. After selection of the best membranes the effect of filtration conditions such as pH was studied and concentration filtrations were made to produce water that could be discharged according to the environmental license of Honkajoki Oy. In addition, a hydrid membrane filtration-evaporation process was studied to fractionate the condensate solution to valuable fractions. A Heidolph Hei-VAP Advantage rotavapor was utilised in evaporation tests. Total organic carbon, conductivity, pH and total and ammonium nitrogen were analysed.

Results and discussion

Membrane modification by ALD

ALD can be used to tailor membrane retention properties as Fig. 1 shows. The 20 kDa UP020 membrane was successfully modified by ALD (86 °C ZnO-N) to a 4 kDa membrane. At the same time the permeability decreased from 34 to 3.5 kg/(m²h bar). The retention of magnesium sulphate was around 60% at the best (Fig. 2). Based on the measured retention values the modified membrane can be classified to belong to tight UF membranes. Although the results showed that the ALD can be used to modify the polymeric membrane properties the modified membrane was too open to separate nutrients from the condensate of Honkajoki Oy and therefore, commercial membranes were used to develop a hybrid process to purify and valorise effluent compounds.

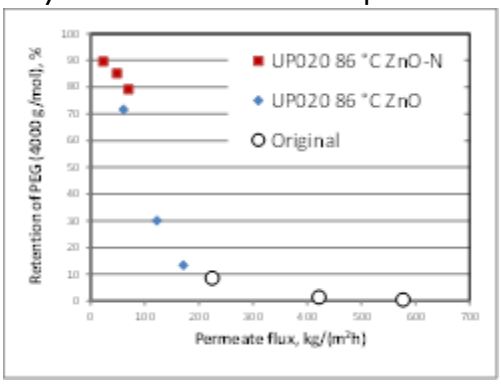

Figure 1 The effect permeate flux (3, 4 and 6 bar) on the retention of coated and virgin UP020 membranes when 200 ppm PEG solution was filtered (ALD1= UP020 86 °C ZnO, ALD2= UP020 86 °C ZnO-N).

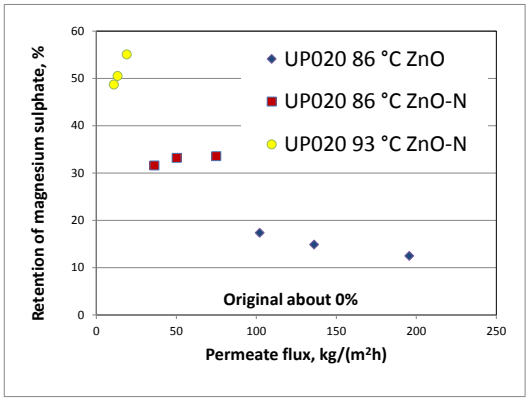

Figure 2 The effect permeate flux (3, 4 and 6 bar) on the retention of coated UP020 membranes when magnesium sulphate water solution was filtered.

Characterization of TiO_2/SiO_2 thin films doped with gold nanospheres and their photocatalytic activity

The TEM image of TiO_2/SiO_2 samples doped with 5 wt% of Au NP is shown on Fig.3.

As it can be seen from the images, spherical shape gold nanoparticles with the average size of 5–7 nm were formed.

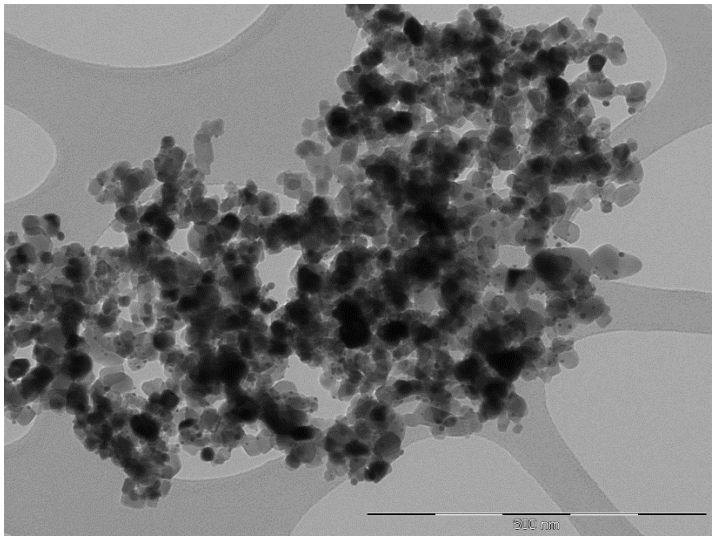

Figure 3 TEM image of TiO_2/SiO_2 film doped with spherical Au NP.

Morphology of the prepared thin films was investigated using SEM images. It was observed that morphology of all coatings is similar. The SEM image of the TiO_2/SiO_2 coating doped with 1.25% of Au NP is presented in Fig.4.

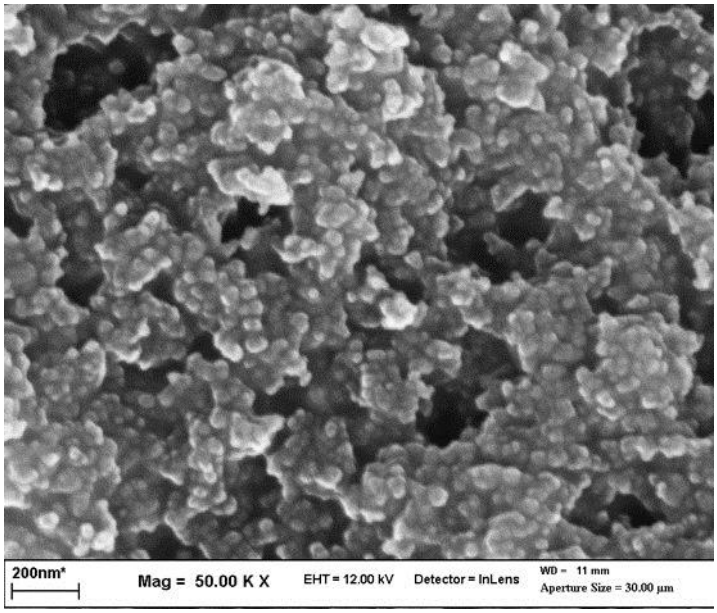

Figure 4 SEM image of TiO_2/SiO_2 film doped with spherical Au NP.

Porosity of the doped coatings was determined after the UVC pretreatment and for Au 0.05%, Au 0.5%, Au 1.25% and Au 5% it was 7.7%, 11%, 9.7% and 14.1%, respectively.

The mean values of contact angle measurements are summarized in Table 1.

Table 1 Contact angle of thin films before and after the UVC pretreatment.

Sample name	Mean contact angle before UVC pretreatment	Mean contact angle after UVC pretreatment
TiO_2/SiO_2 reference	122.3	2.9
TiO_2/SiO_2 Au 0.05%	128.9	3.2
TiO_2/SiO_2 Au 0.5%	129.3	2.7
TiO_2/SiO_2 Au 1.25%	129.3	4.7
TiO_2/SiO_2 Au 5%	99.7	9.9

The results, shown in Table 1, suggest that before and after the UVC pretreatment all the samples exhibit a hydrophobic and super-hydrophilic character, respectively. The hydrophobicity of the prepared coatings after the heat treatment at 120°C can be explained by the presence of organic groups in the thin films. As it was reported earlier for the TiO_2/SiO_2 thin films during the UVC pretreatment photocatalytic degradation of organic groups occurs [3]. Hence, hydrophilicity of coatings drastically increases after the phototreatment.

In order to simplify comparison of photocatalytic performance of different samples and avoid errors caused by deviations in the geometrical area of the samples, the initial FA degradation rates were calculated per cm^2 of the thin film (Fig.5).

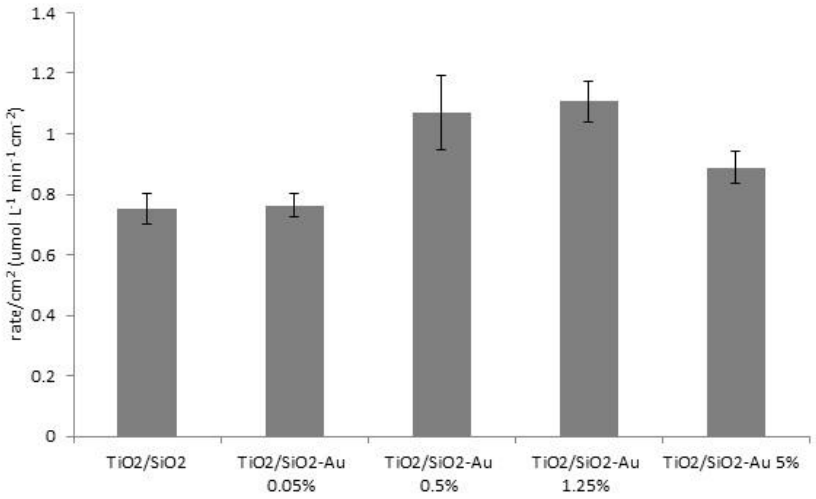

Figure 5 Photocatalytic activity per cm^2 of prepared thin films.

As it can be seen from Fig.5, the initial reaction rates of TiO_2/SiO_2 films doped with 0.5 and 1.25 wt% of Au NP are higher than that of the reference sample and thin films with another loading of Au NP. However, it is difficult to speculate the role of Au NP doping in increased rate constants, other than to note that the loading of TiO_2 is extremely important in this case. Therefore, the areal loadings of TiO_2 NP were measured for all the samples using ICP-OES. The mean areal loadings of TiO_2 varies significantly for thin films doped with a different amount of Au NP. These results suggest that the comparison of photocatalytic activity taking into account only the geometrical surface area can be not representative. Therefore, it was decided to prepare and test TiO_2/SiO_2 thin films with different thicknesses and areal loading of TiO_2 (Fig.6).

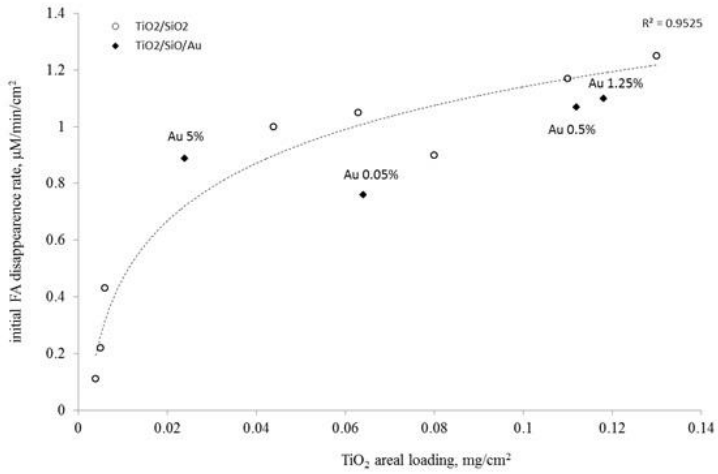

Figure 6 Photocatalytic activity as a function of mean areal loading of TiO_2.

It is worthwhile to note, that photocatalytic activity of coatings doped with gold seems to be not higher than for TiO_2/SiO_2 thin films with similar areal loading of TiO_2. It should be noted that prepared thin films were tested in Visible light only and no photocatalytic activity was detected.

Characterization of TiO_2/SiO_2 thin films doped with gold bipyramid-like nanoparticles and their photocatalytic activity

TEM images of pure Au BP solution and TiO2/SiO2 thin film doped with 1% of Au BP are shown in Fig.7.

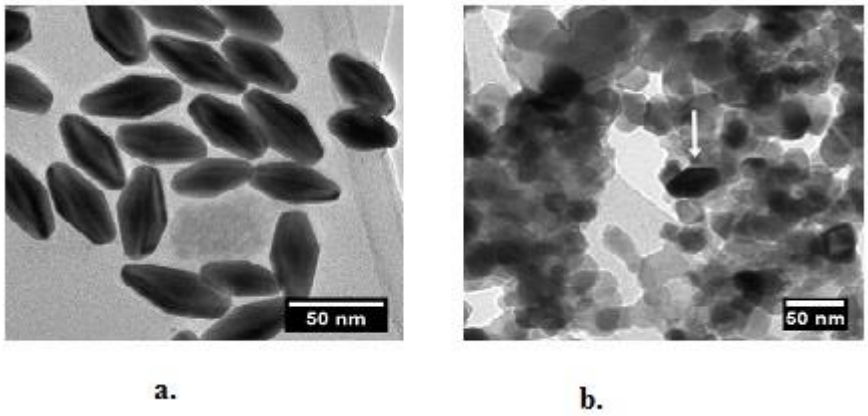

Figure 7 a.TEM of a drop of pure AuBP solution. b. TEM photograph of the 1% AuBP doped film. The white arrow shows a gold bipyramid.

As it can be seen from the figure, size and shape of synthesized AuBP did not undergo significant changes when doped to TiO_2/SiO_2 matrix. Morphology of films doped with Au BP was similar to those doped with Au nanospheres (see Fig.4). Typical XPS spectrum for coatings doped with AuBP is represented in Fig.8.

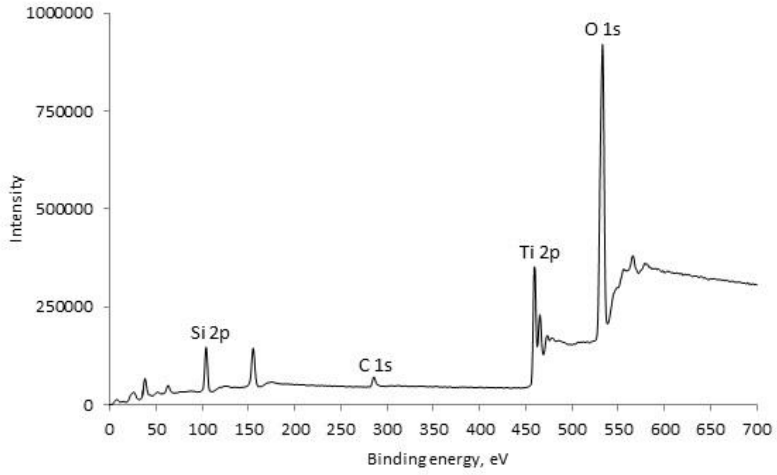

Figure 8 Typical XPS spectrum.

The presence of Au NP was also confirmed by the presence of a detectable Au 4f signal (Fig.9).

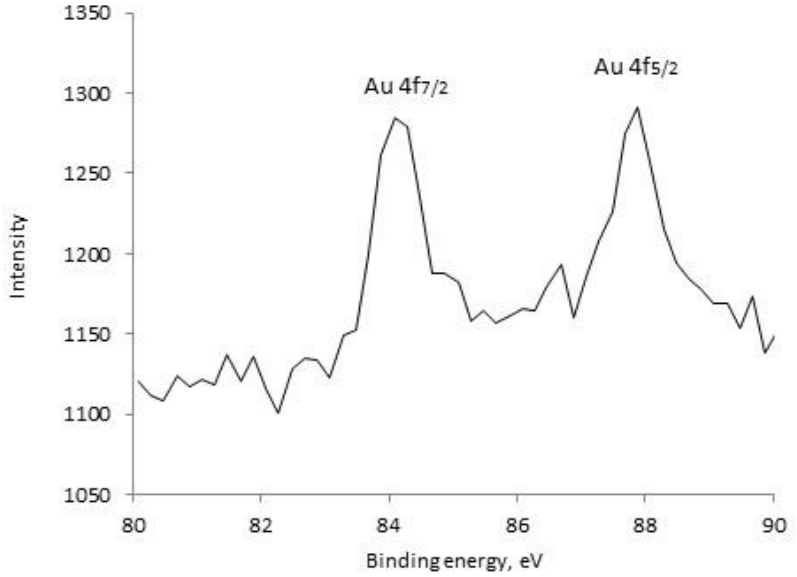

Figure 9 Typical XPS spectrum of Au 4f levels.

The results of the photocatalytic activity of TiO_2/SiO_2 doped with different amounts of Au BP were compared with the reference thin films with a similar areal loading of TiO_2 (Fig.10).

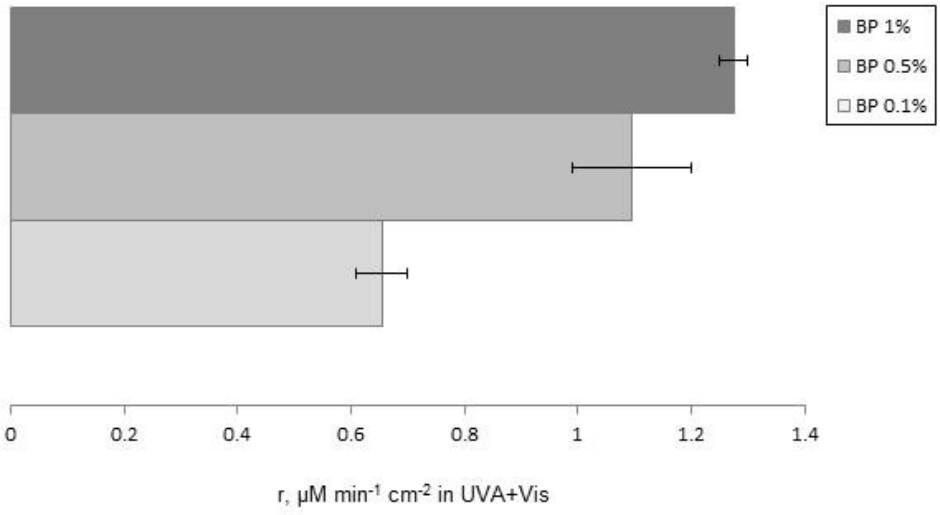

Figure 10 Initial disappearance rate of formic acid for TiO_2/SiO_2/AuBP films with 3 different doping ratios.

The results shown in Fig. 10 shows that with an increased Au loading, the rate rises and photocatalytic activity is improved. The highest initial formic acid disappearance rate is attributed to TiO_2/SiO_2/AuBP 1wt%, which is about two times higher than that of the reference sample with the similar TiO_2 loading. Similar results were reported [4] for degradation of acetic acid in aquatic environment under UV irradiation, which was increased by a factor of 1.7 when the TiO_2 (P25) modified with Au NP (2 wt.%) was compared with bare TiO_2 [4]. Photocatalytic degradation of FA when TiO_2/SiO_2/AuBP 1wt% and TiO_2/SiO_2 (with TiO_2 loading 0.063 mg cm^{-2}) films were used is presented in Figure 11.

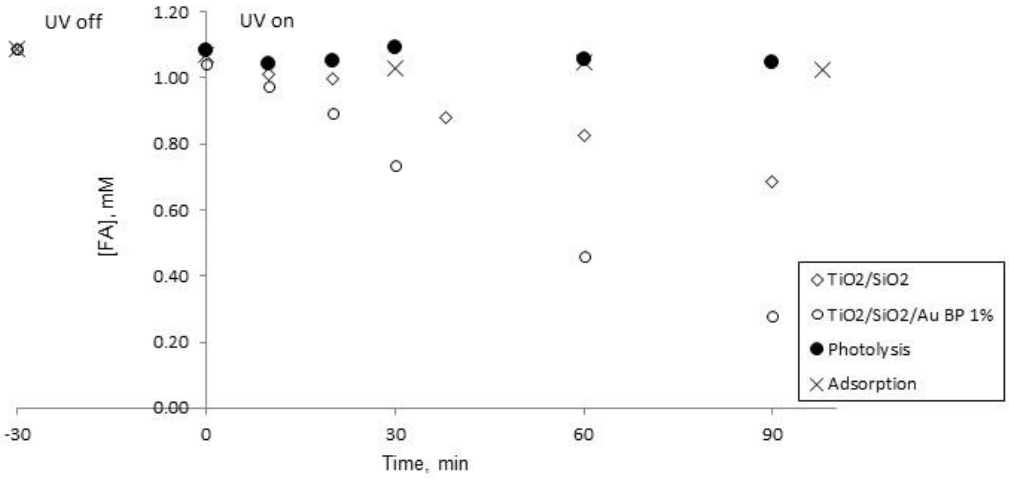

Figure 11 Photocatalytic degradation of formic acid.

As it can be seen from Fig.11, negligible changes in FA concentration were detected during photolysis and adsorption tests. A significant difference in the degradation of FA can be observed for the TiO_2/SiO_2 and TiO_2/SiO_2/AuBP films doped with 1wt% of Au. For instance, after 60 min under UVA+Vis irradiation, 58% of FA was decomposed when the AuBP doped film was used, while for the reference coating this value was only 24%.

Enhanced photocatalytic activity of thin films doped with AuBP can possibly be explained by the fact that gold nanoparticles act as electron traps and promote the electron-hole separation [5-8].

Development of purification process for nutrient rich waste stream

A hybrid process to remove nitrogen compounds from the condensate of Honkajoki Oy was developed. Based on the retention and capacity of the SW30 and NF90 membranes, they were selected to experiments at different conditions. The results showed that a seawater RO membrane (SW30) permeated the ammonium at alkaline conditions. The retention of NH_4+-nitrogen was only 60%. The two pass RO (i.e. filtration of the first stage permeate again) only slightly improved the overall retention of NH_4^+-nitrogen. The final permeate contained NH_4^+-nitrogen almost 300 mg/L but only 50 mg/L organic carbon. Obviously the membrane filtration is not capable to remove enough nitrogen from the condensate solution at alkaline conditions in order to the permeate to be discharged.

Therefore, the condensate pH was adjusted and its effect on the retention was studied. As Fig. 12 shows the pH adjustment from 9.5 to 7 radically improved the retention of NH_4^+-nitrogen. When the pH was decreased further the retention of organic compounds (TOC) also decreased.

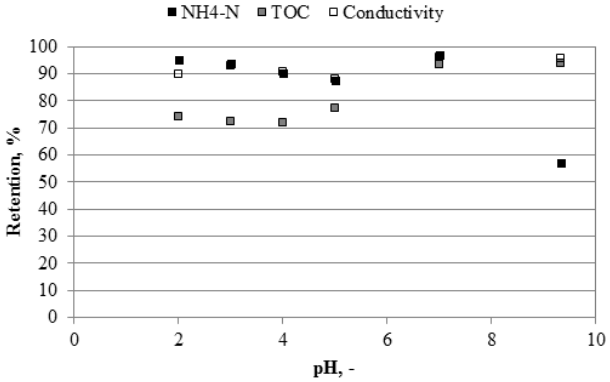

Figure 12 Effect of pH on the retention of the SW30 membrane.

The two pass RO was then made by adjusting pH between the filtration stages. If the pH adjustment is done before the first filtration the retention of nitrogen compounds increases and this increases the osmotic pressure of the solution and decreases the flux. As a result the volume reduction that can be achieved is significantly lower than what was achieved without the pH adjustment (Figure 13 a and b). Therefore, the condensate was first filtered at original pH until the volume reduction of 12 was achieved. The retention of NH_4^+-nitrogen was only 55% but 92% of conductivity and total organic carbon was retained. The permeate solution still contained about 900 mg/L NH_4^+-nitrogen. After adjusting the pH of the permeate to pH 7 the permeate was filtered again using the same membranes. The NH_4^+-nitrogen concentration in the permeate of the second pass RO was only about 40 mg/L (Fig. 14). This is a significantly lower value than is allowed based on the environmental permission of the plant. Therefore, a two pass membrane filtration with the pH adjustment prior to the second filtration produces permeate that can be directly discharged.

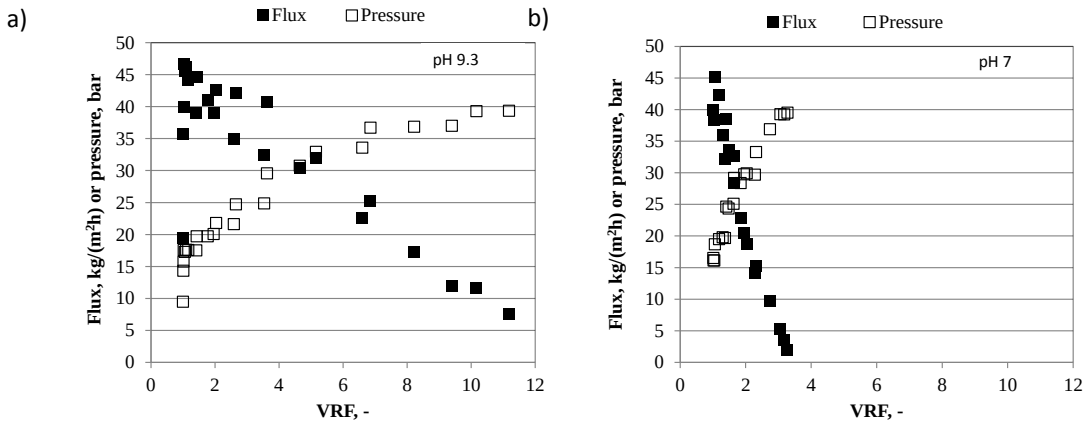

Figure 13 Concentration filtration of original (pH 9.3, a) and pH adjusted (pH 7, b) condensate (SW30 membrane).

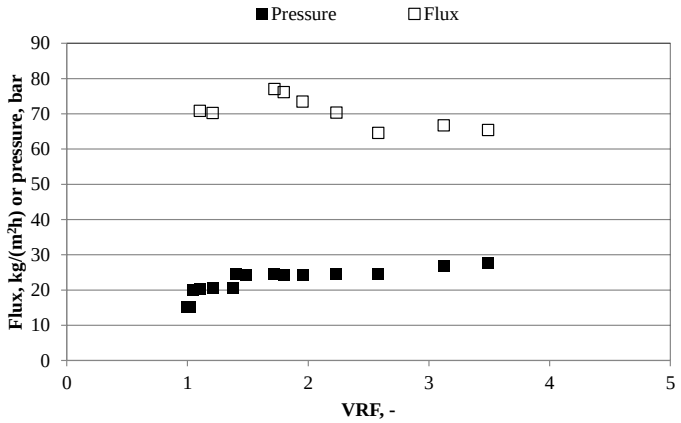

Figure 14 Permeate flux and pressure when the permeate of the first filtration step at original pH was filtered again after pH adjustment to pH 7.

The concentrate steams from membrane filtrations contained both nitrogen compounds and organic acids. These groups can be separated by evaporation or reverse osmosis at acidic conditions. In both cases nitrogen compounds are concentrated and acids permeated or evaporated. Finally the NH_4^+-nitrogen content in the evaporation residue was 76 g/L at volume reduction of 20 in evaporation. The concentration factor of NH_4^+-nitrogen was almost 18. The total organic carbon concentrated less than 3 fold. Therefore, significant separation of nitrogen compounds from the organic matter was achieved. Further characterisation of the produced streams is still needed to evaluate their usability asin fertiliser or chemical industry raw material (organic acid fraction). In addition, a long term performance of the process concepts need to be verified.

References

1. Chateau D, Chaput F, Lopes C, Lindgren M, Brännlund c, Öhgren J, Djourelov N, Nedelec P, Desroches C, Eliasson B, Kindahl T, Lerouge F, Andraud C & Parola S (2012) Silica hybrid sol–gel materials with unusually high concentration of Pt–organic molecular guests: Studies of luminescence and nonlinear absorption of light. ACS Applied Materials & Interfaces 4: 2369-2377.

2. Chateau D, Liotta A, Vadcard F, Navarro J, Chaput F, Lermé J, Lerouge F & Parola S (2015) From gold nanobipyramids to nanojavelins for a precise tuning of the plasmon resonance to the infrared wavelengths: experimental and theoretical aspects. Nanoscale 7: 1934-1943.

3. Gregori D, Benchenaa I, Chaput F, Therias S, Gardette J, Léonard D, Guillard C & Parola S (2014) Mechanically stable and photocatalytically active TiO_2/SiO_2 hybrid films on flexible organic substrates. Journal of Materials Chemistry A 2: 20096-20104.

4. Kowalska E, Mahaney OOP, Abe R & Ohtani B (2010) Visible-light-induced photocatalysis through surface plasmon excitation of gold on titania surfaces. Phys.Chem.Chem.Phys. 12: 2344-2355.

5. Okuno T, Kawamura G, Muto H & Matsuda A (2014) Fabrication of Shape-Controlled Au Nanoparticles in a TiO_2-Containing Mesoporous Template Using UV Irradiation and Their Shape-Dependent Photocatalysis. Journal of Materials Science & Technology 30: 8-12.

6. Liu C, Yang T, Wang C, Chien C, Chen S, Wang C, Leng W, Hwu Y, Lin H, Lee Y, Cheng C, Je JH & Margaritondo G (2009) Enhanced photocatalysis, colloidal stability and cytotoxicity of synchrotron X-ray synthesized Au/TiO_2 nanoparticles. Mater. Chem. Phys. 117: 74-79.

7. Iliev V, Tomova D & Rakovsky S (2010) Nanosized N-doped TiO_2 and gold modified semiconductors — photocatalysts for combined UV–visible light destruction of oxalic acid in aqueous solution. Desalination 260: 101-106.

8. Kaur R, & Pal B (2012) Size and shape dependent attachments of Au nanostructures to TiO_2 for optimum reactivity of Au–TiO_2 photocatalysis. Journal of Molecular Catalysis A: Chemical 355: 39-43.

6 INSTITUTE OF CHEMICAL PROCESS FUNDAMENTALS OF THE CZECH ACADEMY OF SCIENCES, V.V.I. (ICPF CAS)

Lenka Matějová[1,2], Radek Fajgar[2], Olga Šolcová[1]

Institute of Chemical Process Fundamentals of the CAS, v.v.i.
[1]Department of Catalysis and Reaction Engineering
[2]Department of Analytical and Material Chemistry
Rozvojová 135, 165 02 Prague 6-Suchdol, Czech Republic

Dr. Lenka Matějová

Olga Šolcová, DSc.

Abstract
The role of the research group at ICPF CAS within the HYMEPRO project consisted textural and structural characterizations of the prepared low-cost activated carbons (ACs) as well as various types of agro-wastes from which the activated carbons were produced. The revelation of the correlation between the preparation process parameters or agro-wastes' textural properties and textural and structural properties of prepared ACs was a subject of a keen scientific interest. Since the developed ACs were explored in the removal of large molecular-size organic pollutant (methylene blue) and heavy metals (As(V), Pd(II), Cd(II)) from effluents, the molecular dimensions of the model organic pollutant (methylene blue) were estimated via DFT calculations to reveal whether methylene blue can be adsorbed in the micropores of the developed ACs or not. Beside parent raw materials, the following prepared ACs were characterized: (i) ACs from the Finnish pine wood and the Peruvian cocoa pod husk prepared by using various chemical activators and different particle-size of the agro-waste, (ii) $ZnCl_2$-based-ACs produced from two novel raw materials, seeds of red mombin fruit and ice cream-bean, (iii) $ZnCl_2$-based-ACs derived from a broad range of Peruvian agro-wastes (cocoa pod husk, the internal and external parts of mango pits, coffee husk and corn cob) and (iv) ACs derived from the Peruvian cocoa pod husk by using optimal preparation process parameters.

Introduction

Heavy metals and volatile organic compounds (VOCs) which are mainly emitted from technological processes and operations as a part of wastewater or emissions within mining, dye, textile or pharmaceutical industry represent a serious environmental problem because of their harmful and toxic effects on living organisms and human health. Adsorption in a liquid phase as well as in a gas phase belongs to the non-destructive ways how to remove these contaminants and also recover them (Graydon et al. 2009, Rio et al. 2007, Khan & Ghoshal, 2000). Moreover, the adsorbent can be reused after regeneration.

Due to the fact that the amount of heavy metal ions and VOCs uptake on porous materials depend besides others on the internal surface area (Chiang Y.-Ch. *et al.*, 1998), activated carbons (ACs) belong in addition to zeolites to the most used adsorbents. However, AC is traditionally manufactured from non-renewable coal which increases the price as well as the environmental impact. Therefore, there is a need to find alternative, inexpensive, abundant and more environmentally friendly raw materials for adsorbent material production. A wide range of studies have been conducted to reach this aim,

using different agricultural and forest wastes as raw materials. Besides economic benefits, the use of agricultural by-products has environmental advantages (Bhatnagara & Sillanpää, 2010).

Objectives of the research

The research of our group at ICPF within the HYMEPRO project was focused on investigation of textural and structural properties of the low-cost activated carbons prepared from various types of agro-residues. The revelation of the correlation between the preparation process parameters or agro-residues textural properties (*e.g.* their porosity) and textural and structural properties of the prepared ACs was a subject of our keen scientific interest. To reveal the key properties determining the ACs adsorption performance in the removal of large molecular-size organic pollutants, the molecular dimensions of the model organic pollutant (methylene blue) were also estimated via DFT calculations and correlated with textural properties of produced ACs.

Materials and methods

Materials. Produced ACs as well as raw agro-residues or forest-residues for characterization studies were obtained from Minna Pirilä (from the University of Oulu, Finland) or Gerardo Cruz (from the National University of Tumbes, Peru).

Textural properties (*i.e.* specific surface area, micropores up to macropores-size distribution, micropore volume, mesopore surface area, bulk density, skeletal denstity, porosity, total pore volume) of produced ACs as well as raw agro-residues were evaluated from nitrogen and krypton physisorption measurements at 77 K, high-pressure mercury porosimetry and helium pycnometry measurements.

Nitrogen and krypton physisorption measurements at 77 K were performed on the automated volumetric apparatuses ASAP2020 or ASAP2050 Micromeritics (USA). To guarantee the precision of the measured data the highly pure (99.9995%) nitrogen, krypton and helium were used. The high precision of pressure measurements was achieved by using the low pressure transducer with the capacity of 0.1 Torr. The equilibration time was set by several sets of 15-fold repeated pressure measurement covering 10 s. Only after less pressure change than 0.01% between subsequent 15-fold pressure sets was achieved the nitrogen adsorption/desorption point was taken. Before physisorption analysis, the samples of ACs were dried at 350 °C under 1 Pa vacuum for 40 h (for analyses including determination of micropore-size distribution) and at 105 °C under 1 Pa vacuum for 16 h (for standard analyses including the determination of mesopore-size distribution). Concerning agro-residues, the sieved raw agro-residues (particle size 0.5–1 mm) were firstly dried in an oven at 105 °C under ambient pressure for 72 h and then degassed at temperature of 105 °C for 48 h under vacuum less than 1 Pa. The specific surface area, S_{BET}, was evaluated from the nitrogen adsorption isotherm in the range of relative pressure p/p_0 = 0.05–0.25 using the standard Brunauer–Emmett–Teller (BET) procedure (Brunauer *et al.*, 1938). Since the specific surface area, S_{BET}, is not a trustworthy parameter in the case of analysis of porous solids comprising micropores because the BET theory was designed for purely mesoporous or nonporous solids, the mesopore surface area, S_{meso}, and the micropore volume, V_{micro}, were also determined by the t-plot method (DeBoer et al., 1966), using the Lecloux-Pirard standard isotherm (Lecloux *et al.*, 1979, Schneider, 1995). The net pore volume, V_{net}, was determined from the nitrogen adsorption isotherm at maximum relative pressure p/p_0~0.995. The pore-size distribution in mesoporous region was evaluated from the desorption branch of the nitrogen adsorption-desorption isotherm in the range of relative pressure $0.05 < x < 0.995$ by the Barrett–Joyner–Halenda (BJH) method (Barret et al., 1951) via the Roberts algorithm (Roberts et al., 1967), using the carbon standard isotherm and the assumption of the slip-pore geometry. The pore-size distribution in the microporous region was evaluated from the low-pressure part of the nitrogen adsorption isotherms ($10^{-7} < x < 0.05$) by application of the Horvath-Kawazoe solution for the slit-pore geometry. Values of necessary parameters were taken from the Micromeritics software (Micromeritics, 2004).

For some ACs the textural parameters were evaluated from nitrogen physisorption data obtained by a Gemini VII 2390 Surface Area Analyzer (Micromeritics, USA), delivered by the Peruvian colleagues.

The bulk density, ρ_{Hg}, the mercury intrusion pore volume, $V_{intruse}$, and the skeletal density, ρ_{He}, of the processed raw agro-residues were determined by high-pressure mercury porosimetry and helium pycnometry using AutoPore III (Micromeritics, USA) and AccuPyc II 1340 pycnometer (Micromeritics, USA), respectively. Prior to the measurements, the precursors received as non-crushed raw materials were dried in an oven at 105 °C for several days to remove physisorbed moisture. For each raw agro-material the high-pressure mercury porosimetry measurement was carried out at least twice in order to evaluate an average value of porosity because of the inhomogeneity of raw materials. Porosity (ε in %) of the raw agro-residues was calculated according to equation $\varepsilon = (1-\rho_{Hg}/\rho_{He})*100$.

ASAP2020 (Micromeritics, USA)

AutoPore III (Micromeritics, USA)

AccuPyc II 1340 (Micromeritics, USA)

The structure order of the produced ACs was examined using Raman spectroscopy. Raman spectra were collected using a dispersive Nicolet Almega XR spectrometer equipped with Olympus BX 51 microscope. An excitation laser source (473 nm) with an incident power of 5 mW with 256 expositions with 0.5 s duration was used for collecting the spectra. The laser beam was focused to a spot of 0.6 mm in diameter. The incident energy was minimized to avoid thermal effects as a consequence of the laser irradiation. Spectral resolution of the instrument was 1.93 cm^{-1} and the spectrometer was calibrated using a crystalline silicon standard with line at 520 cm^{-1}. The samples during analysis were placed on an aluminium substrate. Raman spectra were taken from several different places within each sample.

Computational methodology (DFT calculations). The molecule optimization for methylene blue (MB) was performed with Gaussian 03 package (Frisch et al., 2004) with B3LYP (Becke, 1993, Lee et al., 1988) hybrid functional and a 6-31+G(d,p) basis set. The vibrational analysis showed that the structure corresponds to local minima in the potential energy surface. Wave functions from the optimized structure were used for the visualization of the contour map of electrostatic potentials by the Multiwfn program (Lu and Chen, 2012). The van der Waals volume was computed by the Monte

Carlo method as implemented in the Multiwfn program. The molecular dimensions in x, y and z-coordinate axis were evaluated based on the graphical output of the Multiwfn program as the maximum values of vnW surface in the individual coordinate axis.

Results

Activated carbons from the Finnish pine wood and the Peruvian cocoa pod husk

Since the nature of biomass and the parameters of individual treatment steps of biomass play the key roles in preparation of microporous ACs, the effect of different biomasses, chemical activators and particle-size fractions on textural properties of produced activated carbons was investigated. Textural properties such as the specific surface area, micropore volume and micropore- and mesopore-size distributions of a set of laboratory-prepared ACs were evaluated based on nitrogen and krypton physisorption measurements at 77 K in order to reveal the best experimental conditions for the production of microporous ACs from Finish pine wood and Peruvian cocoa pod husk.

In this study the low-cost ACs were prepared from cocoa pod husk and residue chars from pine wood gasification and dry distillation processes. Two different chemical activation agents, potassium hydroxide (KOH) and zinc chloride ($ZnCl_2$), two different carbonization temperatures (650 and 800 °C) and two different raw material particle-size fractions (< 0.5 mm and 0.5-1 mm) were used. After preparation the ACs were compared with each other based on their textural properties. The results within this study were reported in a conference paper published in Proceedings of 2nd SkyPro Conference and were presented as a poster.

The effect of biomass nature. Pine wood (Finland) and cocoa pod husk (Peru) were used as source biomasses for the preparation of ACs. Contrary to the raw cocoa pod husk (CPH), the pine wood was for preparation of ACs firstly either pyrolyzed (PW-PC) or gasified (PW-GC), and such prepared materials were subsequently used for chemical activation. All materials were sieved before chemical activation to particle-size fraction of 0.5-1 mm. From Table I it can be seen that while the raw CPH and pyrolyzed PW were non-porous, possessing very low surface areas 0.46 and 0.38 m^2/g, respectively, the initial gasified PW was already mesoporous with ~71 m^2/g (Figure 1).

Table I Textural properties of initial materials (particle-size fraction of 0.5-1 mm) used for preparation of ACs.

Sample	S_{BET} [$m^2\ g^{-1}$]	S_{meso} [$m^2\ g^{-1}$]	V_{micro} [$cm^3_{liq}\ g^{-1}$]	V_{net} [$cm^3_{liq}\ g^{-1}$]	C_{modif} [-]
CPH	0.46	-	-	-	-
PW-PC	0.38	-	-	-	-
PW-GC	70.7	45.1	0.014	0.087	23.0

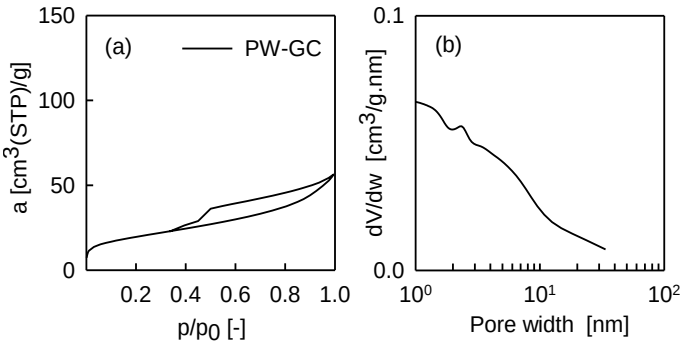

Figure 1 (a) The nitrogen adsorption-desorption isotherm at 77 K and (b) the mesopore-size distribution of PW-GC AC.

Despite the fact that the gasified PW was porous before chemical activation, it did not contribute positively to the evolution of microporous structure of AC via chemical activation by $ZnCl_2$ and carbonization at 650°C (Table 2). On the other hand, micropores were preferentially formed in the pyrolyzed PW and both micropores as well as mesopores were formed in the CPH-based AC (Figure

2, Figure 3). A well-established microporous-mesoporous structure of the CPH-based AC can be seen in Figure 3.

Table 2 Textural properties of ACs prepared from different raw materials, activated by $ZnCl_2$ and carbonized at 650 °C.

Sample	S_{BET} [$m^2\ g^{-1}$]	S_{meso} [$m^2\ g^{-1}$]	V_{micro} [$cm^3_{liq}\ g^{-1}$]	V_{net} [$cm^3_{liq}\ g^{-1}$]	V_{micro}/V_{net} [%]	C_{modif} [-]
CPH-AC	983.9	490.4	0.277	0.734	38	14.3
PW-PC-AC	400.0	43.7	0.179	0.212	84	25.6
PW-GC-AC	111.3	57.5	0.030	0.115	26	15.0

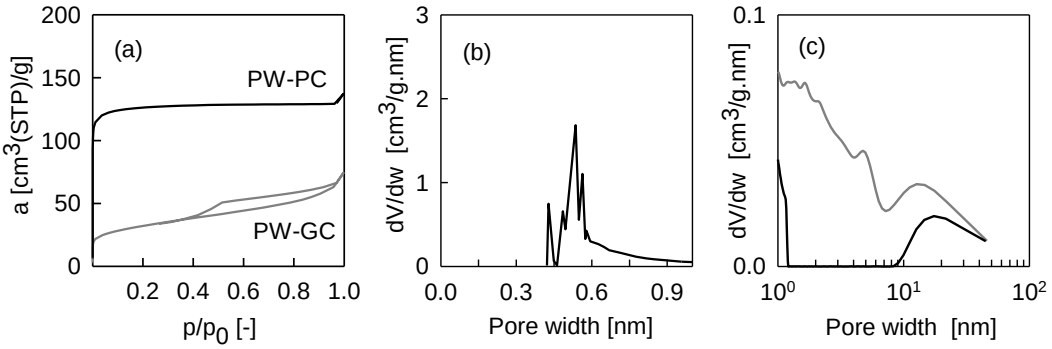

Figure 2 (a) The nitrogen adsorption-desorption isotherms at 77 K of PW-PC and PW-GC ACs, (b) the micorpore-size distribution of PW-PC and (c) the mesopore-size distributions of PW-PC and PW-GC ACs.

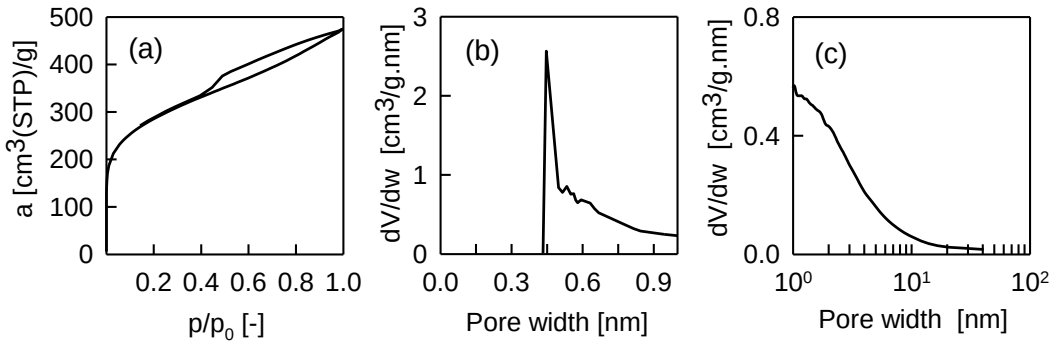

Figure 3 (a) The nitrogen adsorption-desorption isotherm at 77 K, (b) the micropore-size distribution and (c) the mesopore-size distribution of CPH-AC.

The effect of chemical activation. Based on previous knowledge (Cruz *et al.*, 2012) two activation procedures were examined for the preparation of ACs, via (i) $ZnCl_2$ and carbonization at 650°C and (ii) KOH and carbonization at 800°C. It is evident from Table 3 that the activation by KOH/800°C was more effective in the development of ACs porous structure than $ZnCl_2$/650°C and, in general, led to ACs showing higher volume of micropores and mesopore surface area. This effect was more pronounced for the PW-PC based AC than for the PW-GC based AC.

Table 3 Textural properties of PW-based ACs, activated either by $ZnCl_2$/650°C or KOH/800°C; comparison with selected commercial AC.

Chemical activation	Sample	S_{BET} [$m^2\ g^{-1}$]	S_{meso} [$m^2\ g^{-1}$]	V_{micro} [$cm^3_{liq}\ g^{-1}$]	V_{net} [$cm^3_{liq}\ g^{-1}$]	V_{micro}/V_{net} [%]	C_{modif} [-]
$ZnCl_2$, 650°C	**PW-PC**	400.0	43.7	0.179	0.212	84	25.6
	PW-GC	111.3	57.5	0.030	0.115	26	15.0
KOH, 800°C	**PW-PC**	666.6	65.5	0.297	0.346	86	23.2
	PW-GC	218.1	95.3	0.063	0.197	32	23.0

Commercial	**Chem Viron**	775.1	217.3	0.283	0.465	61	23.5

The effect of particle-size fraction. Concerning the different particle-size fractions, it is obvious from Table 4 that using larger particle-size fraction of CPH enhanced the development of a microporous structure of AC activated by KOH. Since KOH is a strong base, the structure of raw materials with particle size < 0.5 mm is destroyed (by digestion) during the carbonization, avoiding the building of porosity.

Table 4 Textural properties of CPH-based ACs, activated by KOH and carbonized at 800°C.

Sample	S_{BET} [$m^2\ g^{-1}$]	S_{meso} [$m^2\ g^{-1}$]	V_{micro} [$cm^3_{liq}\ g^{-1}$]	V_{net} [$cm^3_{liq}\ g^{-1}$]	V_{micro}/V_{net} [%]	C_{modif} [-]
Particle size <0.5 mm	83.5	10.5	0.036	0.087	41	24.6
Particle size 0.5-1 mm	694.7	83.2	0.305	0.381	81	23.3

$ZnCl_2$-based-activated carbons produced from two novel precursors as promising material for application in the treatment of polluted water

In this study the $ZnCl_2$-based ACs from two novel, renewable and up-to-now uninvestigated biomasses, *Spondia Purpurae L.* (red mombin fruit) and *Inga Edulis* (ice cream-bean), were explored. The specific goals were to determine textural and structural properties of both raw agro-residues (separated seeds) and correlate them with those of the produced ACs. Further, the determined properties of the ACs were correlated with their adsorption capacities for methylene blue and arsenic as representative organic and inorganic contaminants in effluents.

Samples of red mombin (*Spondia purpurae L.*) fruit and ice cream-bean (*Inga edulis*) were identified and collected from different areas in Tumbes in the northwest Peru by Gerardo Cruz. The seeds were separated mechanically from the rest of the fruit and bean and were named RMS-RM and GS-RM for red mombin seed and ice cream-bean seed, respectively. The produced ACs were named RMS-AC and GS-AC. The details about preparation of these two ACs are reported in the article 'Cruz at al., $ZnCl_2$-based-activated carbon produced from two novel precursors as promising material for application in the treatment of polluted water' submitted to Journal of Environmental Management in January 2015.

The results from high-pressure mercury porosimetry and helium pycnometry measurements (Table 5, Figure 4) obtained for both raw materials revealed that GS-RM was markedly less porous precursor than RMS-RM. The porosity of GS-RM was very low (~2.5±1%) compared to RMS-RM which possessed the porosity of~44±5 %. On the other side, the repeated analyses revealed that the poor porous structure of GS-RM was more regular than of RMS-RM, and GS-RM comprised beside larger pores as well as smaller pores. The porous structure of RMS-RM was very irregular (Figure 4a). The generally higher porosity of RMS-RM could be more beneficial for the chemical activation, because the activation agent can more penetrate into the internal porous structure of the raw matter particles during the activation step, leading after carbonization to a better established microporous-mesoporous structure of RMS-AC (Table 6, Figure 5).

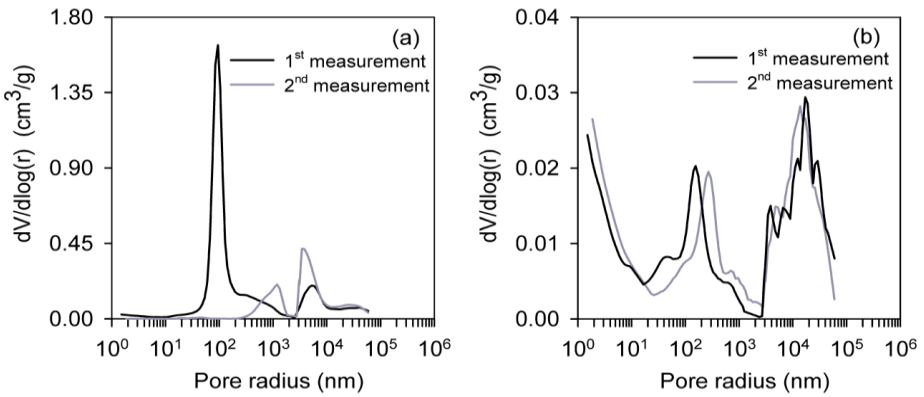

Figure 4 The first and the second measurement of the pore-size distribution of used raw residues from high-pressure mercury porosimetry: (a) RMS-RM and (b) GS-RM.

Table 5 Densities and porosity of the raw residues.

Raw material	ρ_{He} [g·cm^3]	ρ_{Hg} [g·cm^3]	$V_{intruse}$ [cm^3·g]	ε [%]
RMS-RM	1.38	0.72	0.66	44 ± 5
		0.84	0.28	
GS-RM	1.41	1.36	0.05	2.5 ± 1
		1.39	0.05	

The nitrogen adsorption-desorption isotherms measured for the produced ACs and pore-size distributions are shown in Figure 5. The evaluated textural parameters of both produced ACs are summarized in Table 6. It is evident that both produced adsorbents exhibited microporous-mesoporous structure. The shape of nitrogen adsorption-desorption isotherms (Figure 5a) corresponded basically to the type I isotherm according to the IUPAC classification (Gregg and Sing, 1982), typical for microporous materials. Besides that the isotherms included hysteresis loops at higher relative pressures, which are typical for the type IV IUPAC isotherm, indicating the presence of some mesopores. Features of nitrogen adsorption-desorption isotherms corresponded pretty well to the evaluated pore-size distributions shown in Figure 5b. It can be seen that the microporous-mesoporous structure was well established in both adsorbents, but RMS-AC possessed significantly higher mesopore surface area (about ~200 m^2/g) and volume of micropores (about ~132 mm$^3_{liq}$/g) than GS-AC. Concerning the mesopore sizes, GS-AC included a bit wider mesopores than RMS-AC. These features contributed to the explanation of sorption abilities of RMS-AC and GS-AC.

RMS-AC and GS-AC exhibited high S_{BET}, 1405 and 937 m^2/g, respectively. From comparison with those ACs produced from different seeds (taken from literature) was evident that ACs produced in this study possessed significantly higher surface areas than those ACs prepared similarly (by $ZnCl_2$ activation, carbonization at 600°C) by other authors.

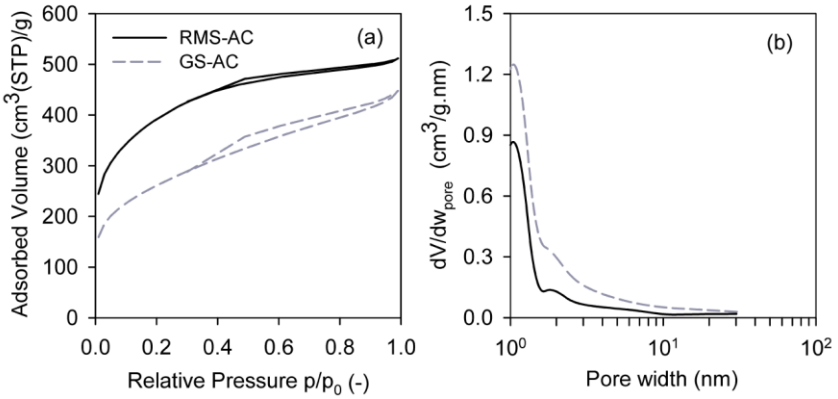

Figure 5 (a) Measured nitrogen adsorption-desorption isotherms and (b) evaluated pore-size distributions of produced RMS-AC and GS-AC.

Table 6 Textural properties of produced RMS-AC and GS-AC.

Activated carbon	S_{BET} [m^2 g^{-1}]	S_{meso} [m^2 g^{-1}]	V_{micro} [cm$^3_{liq}$ g^{-1}]	V_{net} [cm$^3_{liq}$ g^{-1}]	V_{micro}/V_{net} [%]	C_{modif} [-]
RMS-AC	1405	965	0.214	0.792	27	45.0
GS-AC	937	766	0.082	0.693	12	68.7

Raman spectra, characterizing the structure of the GS-AC and RMS-AC (Figure 6), had two broad bands centered at 1358 cm^{-1} (D-band) and 1609 cm^{-1} (G-band), and 1367 cm^{-1} and 1607 cm^{-1}, respectively. The D-band is associated with the disordered carbon structure in amorphous and quasi-crystalline forms of carbon. The G-band corresponds to the E_{2g} mode (stretching vibrations) in the basal plane of the crystalline graphite (Ferrari and Robertson, 2000). It is known, that the width of the

graphitic G-band is related to the degree of graphitization (Yoshida, 2006). It was shown that the interplanar distance of lattice planes of Miller indices (002) of carbon layers strongly depends on the FWHM (full width at half maximum) of the G-band. The FWHM of the G-band corresponding to RMS-AC and GS-AC was 69 cm^{-1} and 77 cm^{-1}, respectively. From the dependence of G-FWHM on interlayer spacing of carbon films (Yoshida et al., 2006) we deduced that d_{002} values of the ACs are greater than 0.343 nm which proved the presence of the turbostratic carbon forms in the produced ACs.

Carbonization of both raw residues was performed at relatively low temperature (600 °C) and the amorphous character of the prepared carbon was dominating above nanocrystalline forms. The position of the G peak is determined by several factors and one of the most important is the hydrogen content. In visible Raman spectra, C-H stretching vibrations lied above 3000 cm^{-1} and the bending modes in the D-peak region. The bending vibration can, however, be neglected because it is not resonantly enhanced (Ristein et al., 1998). In both ACs, the G peak positions were above 1600 cm^{-1}which was an evidence for a low hydrogen content (lower than 20 at.%). Also in the C-H bonding vibration region there was no feature proving the presence of C-H bonds. In this region only the second order of the G band (2G) was located at 3206 and 3202 cm^{-1}, G+D combination vibrations centered at around 2950-2960 cm^{-1} and a broad bump corresponding to 2D vibrations appeared between 2300 and 3200 cm^{-1}.

Concerning the intensity ratio of the band D and G, I_D/I_G is a measure of the zone edges or border phonons of the clusters, which depends on the cluster sizes and distributions (Wagner et al., 1989). The G-band width for RMS-AC and GS-AC was 69 and 77 cm^{-1}, respectively. The corresponding I_D/I_G ratios were 1.61 (RMS-AC) and 1.52 (GS-AC), which meant that cluster sizes are smaller than 1 nm according to the Tuinstra and Koenig equation (Tuinstra and Koenig, 1970).

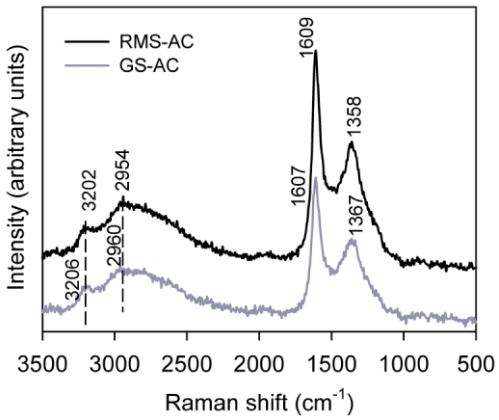

Figure 6 Raman spectra of produced RMS-AC and GS-AC.

Both activated carbons had the ability to adsorb methylene blue and As(V) in aqueous solutions. In the case of the methylene blue removal, both activated carbons reached levels higher than 90% within 1 h, while in the case of the As(V) removal, RMS-AC showed significantly better adsorption performance (close to 100 % in 2 h) than GS-AC (60 % in 2 h). Regards to methylene blue adsorption, the specific surface area and the pores-size distribution played an important role, while for As(V) uptake the ash content played the determining role in adsorption.

A comparative study on activated carbons derived from a broad range of agro-industrial wastes for removal of large molecular size organic pollutants in aqueous-phase

This study aimed to characterize produced ACs from a broader range of agro-industrial wastes. ACs were produced by using the chemical activation with $ZnCl_2$ and carbonization at mild conditions (by Gerardo Cruz from National University of Tumbes, Peru) and were investigated for the removal of model large molecular size organic pollutant in aqueous phase (methylene blue) (by Minna Pirilä from University of Oulu, Finland). A novel raw material in the activated carbon production, external part of the mango pit (mango seed husk), was used. The details about preparation of these ACs are reported in the article 'Cruz at al., A comparative study on activated carbons derived from a broad

range of agro-industrial wastes in removal of large molecular size organic pollutants in aqueous-phase' submitted to the Water, Air and Soil Pollution Journal in February 2015.

The main goal of our study was to reveal the key material properties influencing the ACs adsorption performance for removal of organic pollutants. High-pressure mercury porosimetry and helium pycnometry measurements were performed to characterize the raw lignocellulosic precursors in order to reveal the possible correlation between the porosity of raw agro-material and the quality of produced ACs. Further, all ACs were characterized by nitrogen physisorption at 77 K. In order to prove or disprove the possibility of model organic pollutant to be adsorbed in the micropores of produced ACs or not, the molecular dimensions of model organic pollutant (methylene blue) were estimated via DFT calculations and correlated with textural properties of produced ACs.

Cocoa (*Theobroma cacao*) pod husk (CPH-RM), the internal and external parts of mango (*Manguifera indica*) pits (MSIP-RM and MSEP-RM, respectively), coffee (*Coffea arabica L.)* husk (CH-RM) and corn (*Zea mays*) cob (CC-RM) were collected from different agro-industrial factories and agricultural areas in two cities in the north of Peru, Piura and Tumbes, by Gerardo Cruz. Corresponding ACs produced from individual agro-materials were assigned CPH-AC, MSIP-AC, MSEP-AC, CH-AC and CC-AC.

The results from high-pressure mercury porosimetry and helium pycnometry measurements (Table 7) obtained for individual raw materials revealed that investigated raw materials show significantly different porosity in the broad range of 15–65 %. From all agro-industrial wastes CC-RM was the most porous material (ε ~ 65±1 %) and CH-RM was the least porous material (ε ~ 15±1 %). Concerning raw materials from mango seed, MSEP-RM was about 10 % more porous than MSIP-RM. The overall order in porosity of raw materials was following: CC-RM >CPH-RM >MSEP-RM >MSIP-RM >CH-RM. The fact that the raw material had higher porosity could be important, since higher porosity of the raw material may mean higher surface area being in the contact with activation agent, improving the overall activation process and thus resulting in activated carbons with well-developed microporous-mesoporous structure possessing higher surface areas. According to the repeated high-pressure mercury porosimetry measurements (Figure 7, Table 7) MSEP-RM, CH-RM and CC-RM were relatively homogeneous materials and had regular porous structure within pore sizes 0.002–4 μm contrary to CPH-RM and MSIP-RM which were either inhomogeneous (CPH-RM) or homogeneous with irregular porous structure (MSIP-RM). From PSD curves in Figure 7 it was evident that CC-RM in contrast to other raw precursor materials had dominantly larger uniform pores. MSEP-RM, MSIP-RM, CPH-RM and CH-RM showed pores of wide range of sizes. From Table 7 it can be also seen that all raw materials showed very low surface areas, within the range 0.29–0.44 m^2/g.

Table 7 The density and porosity of agro-industrial wastes as-received and the specific surface area of agro-industrial wastes sieved to particle size fraction of 0.5–1 mm.

Raw material	ρ_{He} [g·cm^3]	ρ_{Hg} [g·cm^3]	$V_{intruse}$ [cm^3·g]	ε [%]	S_{BET} [m^2·g]
MSEP-RM	1.39	0.89 0.83	0.40 0.56	38 ± 2	0.29
MSIP-RM	1.40	1.04 1.02	0.32 0.30	27 ± 1	0.31
CPH-RM	1.43	0.53 0.95	0.39 0.40	48 ± 16	0.44
CH-RM	1.33	1.14 1.13	0.15 0.19	15 ± 1	0.40
CC-RM	1.28	0.45 0.46	1.40 1.56	65 ± 1	-

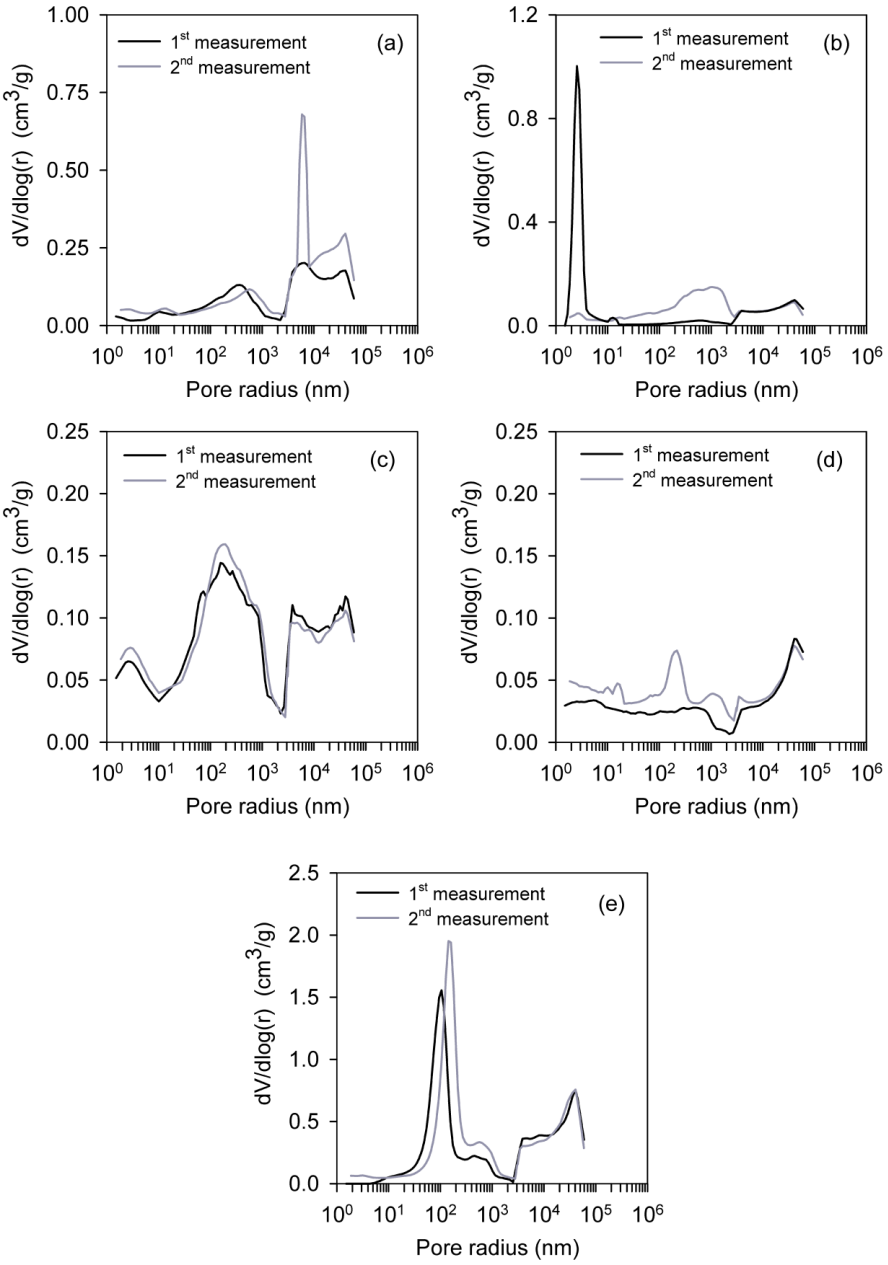

Figure 7 Pore-size distributions of raw agro-industrial wastes determined by high-pressure mercury porosimetry; (a) MSEP-RM, (b) MSIP-RM, (c) CPH-RM, (d) CH-RM and (e) CC-RM.

The shape of nitrogen adsorption-desorption isotherms of produced ACs in this study (Figure 8a,b,c) corresponded basically to the I type isotherm according to the IUPAC classification (Gregg and Sing, 1982), typical for microporous materials. Besides that the isotherms included hysteresis loops at higher relative pressures, which are typical for the IV type IUPAC isotherm, indicating the presence of mesoporous structure. According to Figure 8 and Table 8, all activated carbons produced from lignocellulosic agro-industrial wastes exhibited a well-developed microporous-mesoporous structure. However, there can be seen several significant differences. CC-AC showed significantly higher mesopores surface area (~618 m^2/g) than other ACs (503–561 m^2/g), but not so high micropore volume. Concerning mango seed produced ACs, MSIP-AC showed very similar porous structure morphology as MSEP-AC, but was slightly more porous. CPH-AC and CH-AC also possessed practically the same porous structure morphology. The micropore volume of individual ACs was decreasing in following order: CPH-AC ~ CH-AC > MSIP-AC ~ CC-AC > MSEP-AC. CC-AC comprised the most uniform mesopores. Micropore size distributions (Figure 9) of CPH-AC, MSIP-AC, MSEP-AC and CH-AC revealed that produced activated carbons have very similar irregular microporous structure. ACs comprised smaller and larger micropores with pore-sizes 0.4–0.45 nm and above ~0.48 nm, respectively. In general, the pore size-distributions of the activated carbons might

be the determining parameter in the case of polluted water and wastewater treatment, because of the possible fast access for low and high molecular-weight molecules of pollutants through macropores and mesopores to reach micropores, improving thus the adsorption properties of developed adsorbent (Galiatsatou et al.,2001).

Linear regression models were conducted in order to study the relationship between the porosity (ε) of the raw material and the S_{meso} and V_{micro} of the produced activated carbons. Since the calculated correlation coefficients of the models were low, no direct relationship between the porosity, ε, of original raw agro-material and the textural properties such as a surface area or micropore volume of developed ACs can be proved. On the other side, it was evident that the utilization of a raw agro-material possessing dominantly uniform macropores of ~300 nm pore-size and of large volume (Figure 7e, Table 7) results in AC showing the well-developed mesoporous structure, having the highest mesopore surface area and channel-like pore morphology (Table 8, Figure 8f), which is the case of CC-RM. Thus, it could be concluded that the pore-size distribution of raw agro-material plays more important role in developing of microporous-mesoporous ACs than their overall porosity. It affects the level of interaction of an activation agent with a lignocellulosic material. In general, the raw materials showing wide range of pore sizes and higher ratio of larger pores within mesoporous-macroporous structure allows developing of the activated carbons with high surface areas.

Table 8 Textural properties of the produced ACs.

Activated carbon	S_{BET} [$m^2 g^{-1}$]	S_{meso} [$m^2 g^{-1}$]	V_{micro} [$cm^3_{liq} g^{-1}$]	V_{net} [$cm^3_{liq} g^{-1}$]	V_{micro}/V_{net} [%]	C_{modif} [-]
MSEP-AC	939	504	0.221	0.602	37	19.0
MSIP-AC	1094	561	0.266	0.691	38	19.0
CPH-AC	1162	503	0.322	0.726	44	23.9
CH-AC	1135	518	0.305	0.732	42	20.8
CC-AC	1121	618	0.250	0.657	38	21.5

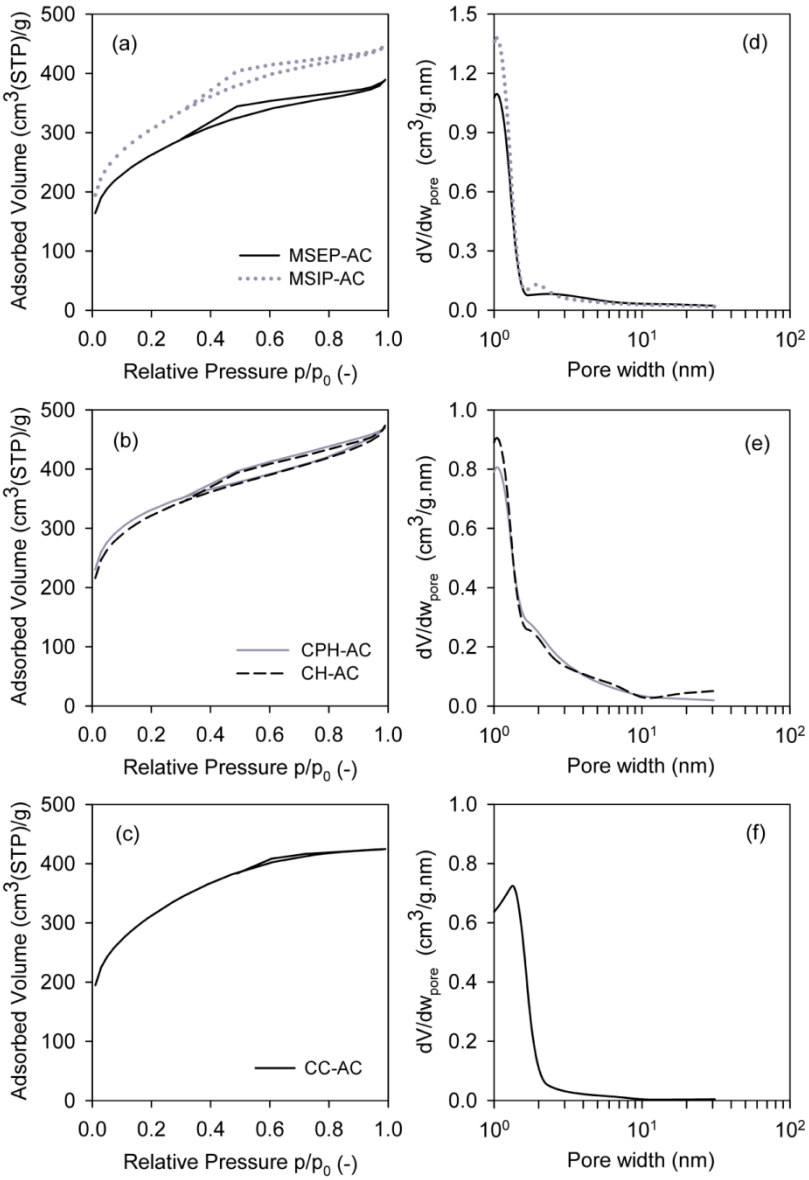

Figure 8 (a,b,c) Measured nitrogen adsorption-desorption isotherms and (d,e,f) evaluated pore-size distributions of produced ACs.

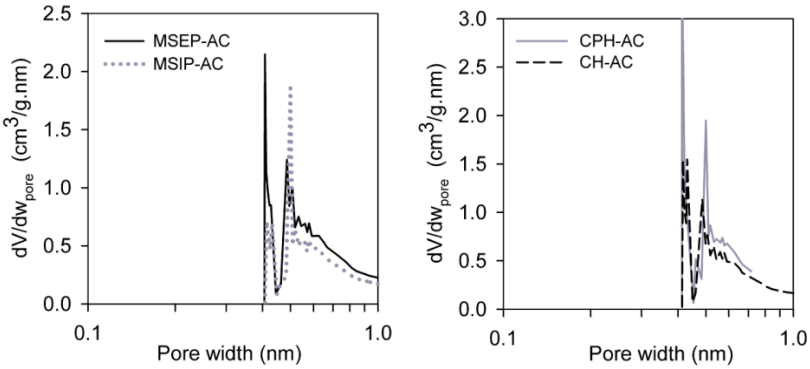

Figure 9 Evaluated micropore-size distributions of produced ACs. Data for CC-AC are not available.

Considering the molecular dimensions of methylene blue (MB) from our estimation via DFT calculations (1.66 x 0.82 x 0.54 nm, Figure 10) it seems, that this pollutant can diffuse and be adsorbed the most likely in mesopores of CC-AC. Since mesopore-size distributions of other activated carbons are quite similar (Figure 8d, e), the transport of methylene blue within the mesoporous structure will be more or less similar, resulting thus to a similar adsorption behaviour of ACs.

Secondly, the size selectivity of the micropores with respect to dimensions of methylene blue molecule is also the factor which had to be considered. It can be reasonably supposed that the adsorption of MB could not occur on the whole micropore surface of the activated carbons. This assumption was in agreement with molecular simulations of MB. It is evident from Figure 10, that MB due its dimensions may be adsorbed only in larger micropores (with size > 0.54 nm) in all ACs. From Table 8 it is evident that CPH-AC showed the highest micropore volume. Since all ACs possessed practically the same micropore-size distribution (Figure 9), however, CPH-AC possessed the highest micropore volume of 322 mm^3_{liq}/g (Table 8), the highest adsorption within the micropores can be expected for CPH-AC. Based on all above mentioned facts it seems that the best adsorption performance for MB reached on CC-AC and CPH-AC can be attributed to the well-developed mesoporous structure of CC-AC, showing the highest mesopore surface area. When the mesopore surface areas of ACs were similar, than the best adsorption performance for MB can be attributed to the contribution of available micropore volume which was the highest for CPH-AC.

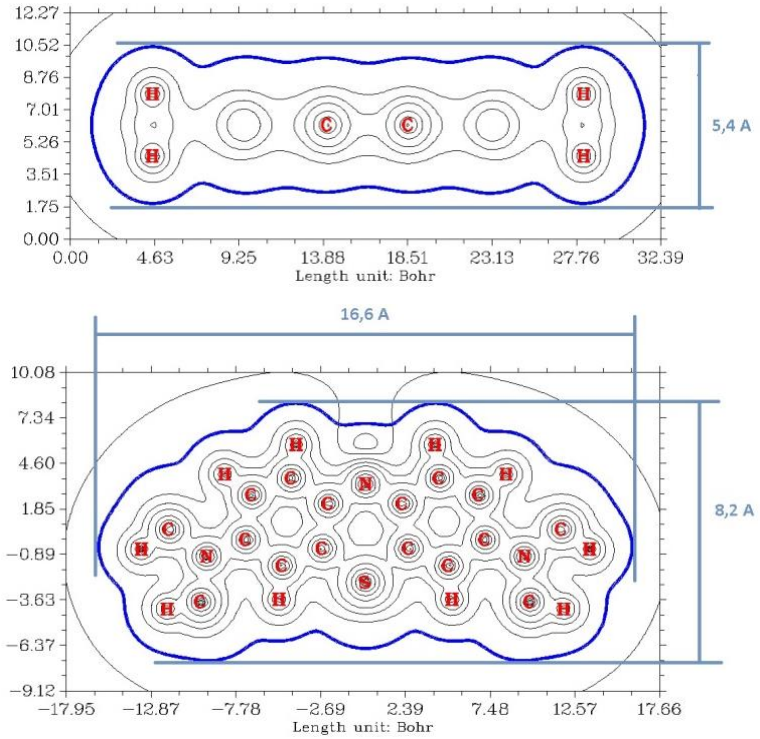

Figure 10 The contour map of electrostatic potential in xy-axis and xz-axis planes of methylene blue. The bold blue line corresponds to the vdW surface (isosurface of electron density = 0.001 a.u.). 1 bohr = 0.529 Å.

Activated carbons derived from cocoa pod husk for removal of As(V), Cd(II) and Pb(II) from multicomponent aqueous systems

These ACs were characterized, since they were explored in removal of As(V), Cd(II) and Pb(II) in multicomponent aqueous systems (by Minna Pirilä from University of Oulu, Finland). CPH-21 AC was prepared from raw material with particle size of 0.5–1 mm and at 500 °C activation temperature. CPH-22 AC was prepared from raw material with particle size of 0.2–0.5 mm and at 650 °C activation temperature. More details about preparation of these ACs are reported in the article 'Pirilä at al., Removal of As(V), Cd(II) and Pb(II) from multicomponent aqueous systems using activated carbons' submitted to the Water, Air and Soil Pollution Journal in April 2015.

Based on the shapes of nitrogen adsorption-desorption isotherms (Figure 11) it can be seen that all investigated ACs possessed microporous-mesoporous structure, exhibiting significant amount of micropores (Table 9). However, while the volume of micropores was comparable in Chemviron and CPH-22 (0.283 cm^3_{liq}/g and 0.288 cm^3_{liq}/g), CPH-21 showed significantly lower volume of micropores of 0.183 cm^3_{liq}/g. The mesopore surface area (surface area of mesopores and macropores) and net pore volume of ACs decreased in the order: CPH-22 > CPH-21 > Chemiviron. Considering the mesopore- and macropore-size distributions, they were more or less indentical for all ACs (Figure 11).

Based on textural results it is evident that the different particle size processed and the activation temperature used during preparation of CPH-derived ACs played a significant role, as the differences in textural properties of CPH-21 and CPH-22 are substantial.

Table 9 Textural properties of commercial Chemviron and prepared CPH-derived ACs (less than 0.25 mm particle size).

Activated carbon	S_{BET} [$m^2\ g^{-1}$]	S_{meso} [$m^2\ g^{-1}$]	V_{micro} [$cm^3_{liq}\ g^{-1}$]	V_{net} [$cm^3_{liq}\ g^{-1}$]	V_{micro}/V_{net} [%]	C_{modif} [-]
Chemviron	775	217	0.283	0.465	61	23.5
CPH-21	709	360	0.183	0.498	37	23.5
CPH-22	1117	568	0.288	0.727	40	23.0

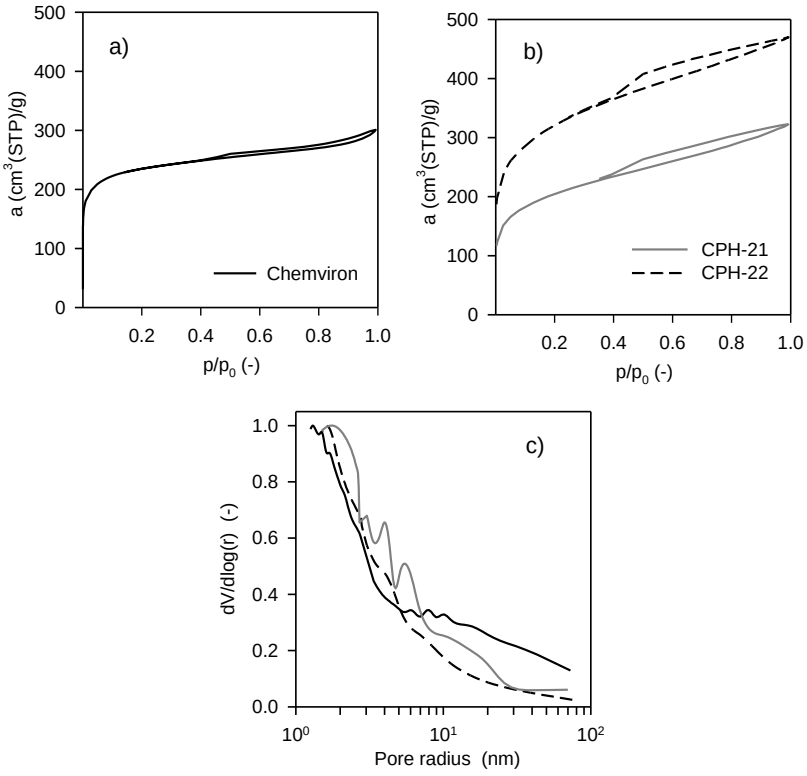

Figure 11 (a,b) Measured nitrogen adsorption-desorption isotherms and (c) evaluated pore-size distributions of investigated Chemviron and CPH-derived ACs.

Relevance of the research

With respect to the removal of heavy metals and metalloids in effluents, the development of efficient and low-cost adsorbents from renewable sources currently represents an important topic under a keen scientific research. The determined textural and structural properties of adsorbents can contribute to explanation their adsorption efficiency.

Papers

Pirilä M, Cruz G, Matějová L, Ainassaari K, Solis J, Šolcová O & Keiski RL (2013) Towards low-cost activated carbons as promising adsorbents. Proceedings. Oulu: University of Oulu. - (Pitkäaho, S.; Pruikkonen, H.; Pongrácz, E.; Keiski, R.L.) S. 111-115. ISBN 978-952-62-0292-1. [Conference: 2nd SkyPro Conference - Clean Air Research at the University of Oulu. Oulu (FI), 12.11.2013].

Cruz GJF, Pirilä M, Matějová L, Ainassaari K, Solis JL, Fajgar R, Šolcová O & Keiski RL (2015) $ZnCl_2$-based-activated carbon produced from two novel precursors as promising material for application in the treatment of polluted water. Journal of Environmental Management, submitted January 2015 (currently under review).

Cruz GJF, Matějová L, Pirilä M, Ainassaari K, Canepa CA, Solis J, Cruz JF, Šolcová O & Keiski RL (2015) A comparative study on activated carbons derived from a broad range of agro-industrial wastes in removal of large molecular size organic pollutants in aqueous-phase. Water, Air and Soil Pollution, submitted February 2015 (currently under review).

Pirilä M, Cruz GJF, Ainassaari K, Gomez M, Matějová L & Keiski RL (2015) Removal of As(V), Cd(II) and Pb(II) from multicomponent aqueous systems using activated carbons. Water, Air and Soil Pollution, submitted April 2015.

Acknowledgements

The financial supports of the Finnish Funding Agency for Innovation (Tekes) (HYMEPRO project, reg. No. 40262/11), the Academy of Sciences of the Czech Republic and Consejo Nacional de Ciencia, Tecnologia e Innovación Tecnológica (CONCYTEC) in Peru (joint project reg. No. 002/PE/2012) are gratefully acknowledged. Authors also thank Hana Šnajdaufová for technical support and Dr. Tomáš Strašák for DFT calculations, both from ICPF CAS (Prague, Czech Republic).

References

ASAP 2020 Operator´s Manual, Micromeritics Instrument Corporation, 2004.

Barret EP, Joyner LG & Halenda PB (1951) The determination of pore volume and area distributions in porous substances. I. Computations from nitrogen isotherms, Journal of American Chemical Society 73: 373-380.

Becke ADJ (1993) Density functional thermochemistry. III. The role of exact Exchange. Chemical Physics 98: 5648−5652.

Bhatnagara A & Sillanpää M (2010) Utilization of agro-industrial and municipal waste materials as potential adsorbents for water treatment - A review. Chemical Engineering Journal 157: 277-296.

Brunauer S, Emmett PH & Teller E (1938) Adsorption of gases in multimolecular layers. Journal of American Chemical Society 60: 309-319.

Chiang Y-Ch, Chiang P-Ch & Chang E-E (1998) Comprehensive approach to determining the physical properties of granular activated carbons. Chemosphere 37 (2): 237-244.

Cruz G, Pirilä M, Huuhtanen M, Carrión L, Alvarenga E & Keiski RL (2012) Production of activated carbon from cocoa (Theobroma cacao) pod husk. Journal of Civil and Environmental Engineering 2:109.

DeBoer JB, Lippens BC, Linsen BG, Broekhoff JCP, Heuvel AVD & Osinga ThJ (1966) The t-curve of multimolecular N_2-adsorption. Journal of Colloid and Interface Science 21: 405-414.

Ferrari AC & Robertson J (2000) Interpretation of Raman spectra of disordered and amorphous carbon. Physical Reviewes B61(20): 14095–14107.

Frisch M, Trucks GW, Schlegel H, Scuseria GE, Robb MA, Cheeseman JR, & Dannenberg JJ (2004) Gaussian 03, revision c. 02; Gaussian. Inc., Wallingford, CT, 4.

Galiatsatou P, Metaxas M & Kasselouri-Rigopoulou V (2001) Mesoporous activated carbon from Agricultural byproducts. Mikrochimica Acta 136: 147-152.

Graydon JW, Zhang X, Kirk DW & Jia CQ (2009) Sorption and stability of mercury on activated carbon for emission control. Journal of Hazardous Materials 168:
978–982.

Gregg SJ & Sing KSW (1982) Adsorption. Surface Area and Porosity. Academic Press, New York, 1982.

Khan FI & Ghoshal AKr (2000) Removal of Volatile Organic Compounds from polluted air. Journal of Loss Prevention in the Process Industries 13: 527–545.

Lecloux A & Pirard JP (1979) The importance of standard isotherms in the analysis of adsorption isotherms for determining the porous texture of solids. Journal of Colloid and Interface Science 70: 265-281.

Lu T & Chen F (2012) Multiwfn: A multifunctional wave function analyzer. Journal of Computational Chemistry 33: 580–592.

Rio S, Verwilghen C, Ramaroson J, Nzihou A & Sharrock P (2007) Heavy metal vaporization and abatement during thermal treatment of modified wastes. Journal of Hazardous Materials 148: 521–528.

Ristein J, Stief RT, Ley L & Beyer W (1998) A comparative analysis of AC:H by infrared spectroscopy and mass selected thermal effusion. Journal of Applied Physics 84(7): 3836–3847.

Roberts BF (1967) A procedure for estimating pore volume and area distributions from sorption isotherms. Journal of Colloid and Interface Science 23: 266-273.

Schneider P (1995) Adsorption isotherms of microporous-mesoporous solids revisited. Applied Catalysis A 129: 157-165.

Tuinstra F & Koenig JL (1970) Raman spectrum of graphite. Journal of Chemical Physics 53 (3): 1126–1130.

Wagner J, Ramsteiner M, Wild C. & Koidl P (1989) Resonant Raman scattering of amorphous carbon and polycrystalline diamond films. Physical Reviewes B, 40(3): 1817–1824.

Yoshida A, Kaburagi Y & Hishiyama Y (2006) Full width at half maximum intensity of the G band in the first order Raman spectrum of carbon material as a parameter for graphitization. Carbon 44(11): 2333–2335.

Yoshida T, Yamauchi H & Sun GF (2004) Chronic health effects in people exposed to arsenic via the drinking water: dose–response relationships in review. Toxicology and Applied Pharmacy, 198: 243–252.

7 UNIVERSIDAD NACIONAL DE INGENIERÍA, LIMA AND UNIVERSIDAD NACIONAL DE TUMBES, TUMBES, PERU

Gerardo J.F. Cruz, Monica M. Gomez and Jose L. Solis

Abstract
Different activated carbons (via chemical activation with $ZnCl_2$) with high surface areas were obtained from abundant inexpensive agrowastes produced in Peru. They were chemically activated with $ZnCl_2$ and carbonized at 600 °C during 2 h in an inert nitrogen atmosphere. The activated carbons produced were able to adsorb methylene blue (MB) in different levels, however activated carbon from corncob (CC-AC) showed the best MB adsorption levels reaching values close to 90% of adsorption in 30 min. A high content of ash in the activated carbons indicate the presence of impurities evolved from the chemical activator.

Three sample of activated carbons, derived from corncob (CC-AC), coffee husk (CH-AC) and the external part of mango pit (MSEP-AC), were used to adsorb As and Pb form samples of polluted Tumbes river water. The materials exhibited high levels of As and Pb removal (close to 90% in only a few minutes), even similar or higher in some cases than that of the commercial activated carbon (Chemvirom)

Introduction

Raw materials in developing countries such as Peru are processed in primary and/or secondary levels, generating significant amounts of wastes that are usually composed of organic matter with different biodegradability. Despite there are different alternatives to use them, only a fraction is recycled as animal food, in production of organic fertilizers or production of energy. The rest is disposed in illegal or legal dumps or burnt generating greenhouse gases and impacting the surrounding environment. The amount of waste produced by agro-industrial activities in Peru is excessive.

One of the feasible alternatives to recycle such residues, according to their content of lignocellulosic compounds, is as precursors for the production of activated carbon, a material with a high surface area suitable for adsorption and catalytic applications. The traditional materials for activated carbon production (such as wood, lignin, coal, etc.) could be replaced for those cheap and renewable residues to reduce costs and to improve the sustainability of the production processes.

Despite of the fact that there is a wide range of studies about the production of activated carbons for different water treatment applications, the interest to produce activated carbon from cheap and renewable raw materials showing a high surface area and special properties for specific applications is still increasing.

The problems in Latin America related to water pollution are linked to organic and inorganic pollutants. Between organic contaminants, the occurrence of dyes in wastewaters is a significant problem, since many dyes are toxic and thus harmful for humans and for the environment. In fact, textile wastewaters are considered as the most polluting among all industrial sectors when considering both the discharge volumes and wastewater compositions. In addition to that, one of the most important groups of inorganic pollutants is heavy metals and metalloids. Thus, drinking water sources contaminated by arsenic are a worldwide concern, considering the fact that it may occur naturally or as a consequence of human activities such as mining operations.

Objective of the research

The goal of the research done in Peru was to

- Produce and characterize activated carbons with high surface area from agrowastes as potential adsorbents
- Determine the adsorption properties of the produced activated carbons with pollutants in liquid phase

Experimental

Agro-waste precursors used for activated carbon production

Code	Description	Scientific name of the material (fruit/bean, etc.)
RMS	Red Mombin seed	***Spondias purpurae*L.**
GS	Ice-cream bean	***Inga edulis***
CC	Corncob	***Zea mays***
MSEP	External part of the mango pit	***Manguifera indica***
MSIP	Internal part of the mango pit	***Manguifera indica***
CPH	Cocoa pod husk	***Theobroma cacao***
CH	Coffee husk	***Coffea arabica L.***

Production of activated carbon from agro-waste

Different agro-waste precursors were washed repeatedly with plenty of water and dried at 100 °C until they had a constant weight, then they were ground and sieved to obtain a 0.5 – 1 mm particle size. $ZnCl_2$ was mixed with the ground raw materials in a 1/1 weight proportion under dry conditions.

The mixture was pyrolysed directly at 600°C using a furnace under nitrogen atmosphere with a flux of about 150 ml/min. A heating rate of 10°C/min was used to reach the final pyrolysis temperature and the samples were kept for two hours and then cooled down to room temperature.

After the pyrolysis, samples were repeatedly washed with a solution HCl of approximately 0.15 N and distilled water at room temperature. Finally all samples were dried at 100 °C overnight, ground and sieved with a mesh of 0.25 mm pore size. This procedure has been used in previous studies [1] and is described in the Figure 1.

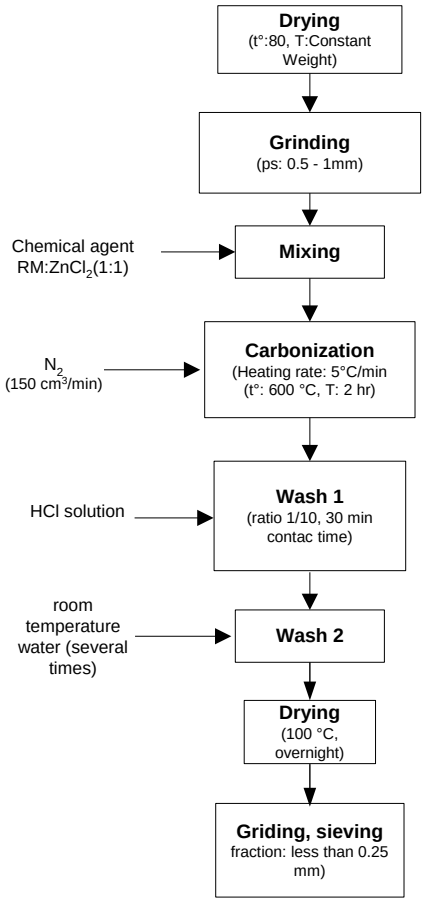

Fig. 1. Procedure for activated carbon production from the different precursors.

Activated carbon characterization

Proximate analysis consisted of moisture (wt.%), dry matter (wt.%) and ash content (wt.%) determinations. The moisture content was determined using the ASTM D2867-04 method and for the ash content, the ASTM D2866-94 (reapproved 2004) method was performed. This method considers the calculation of the ash content in dry basis using calcination temperatures of 600 ± 25 °C during several hours until a constant weight is reached. The difference between 100% and the moisture content (wt.%) gave the dry matter content (wt.%). In Table 1 the proximate analysis results are shown.

Nitrogen physisorption was used in order to determine textural parameters of the produced ACs. The nitrogen physisorption measurements at 77 K were performed on a Gemini VII 2390 surface area analyzer (Micromeritics, USA). Then the information of nitrogen physisorption measurements was studied by PhD. Lenka Matejova in the IFQP-Czech Republic. The pore shape and pore morphology were studied using FE-SEM images from a field emission scanning electron microscope Zeiss Ultra plus.

Methylene blue adsorption tests

Adsorption experiments were carried out to test methylene blue (MB) adsorption capacity of the produced activated carbons. The experiments were conducted without pH adjustment (the initial pH level was between 5.5 and 6.5) and at room temperature between 20 and 25 °C. The activated carbons concentration was 0.5 g/L and the initial MB concentration was 50 mg/L in 200 ml batch. The solutions were shaken in a magnetic stirrer during the experiments. Filtered liquid aliquots were extracted at the beginning and at different times between 5 and 150 min. The MB concentration was determined at the 660 nm wavelength on a Spectroquant Pharo 300 UV-VIS spectrophotometer (Merck).

A pseudo-second order kinetic model (Ho and McKay, 1999) was applied to describe the behavior of MB adsorption data. The integral form of that model can be written as follows:

$$\frac{t}{q_t} = \frac{1}{k_2 q_e^2} + \frac{t}{qe} \qquad (3)$$

where t is the adsorption time (min), q_t is the amount adsorbed at time *t* (mg of adsorbate/g of activated carbon), k_2 is the pseudo-second-order rate constant (g/mg.min) and q_e is the calculated equilibrium adsorption capacity (mg of adsorbate/g of activated carbon). The amount of adsorbate adsorbed at time *t* was calculated by using the following mass balance equation:

$$q_t = \frac{(C_0 - C_t)V}{m_{AC}} \qquad (4)$$

where C_0 and C_t are the initial adsorbate concentration and the adsorbate concentration in solution at time *t* (mg/l), respectively, *V* is the total volume of solution (l) and m_{AC} is the mass of activated carbon (g).

Adsorption tests with the real Tumbes river water

Different activated carbons were produced from corncob (CC-AC), external part of the mango pit (MSEP-AC) and coffee husk (CH-AC) with an improved washing step. Experiments were conducted in order to determine the As and Pb adsorption capacity in real river water (sample from the Tumbes river – Peru) of the those three samples. Samples of 200 ml of water (around pH 6) were put in a 250 ml flask and then shaken in an orbital shaker and the 1 g/l of activated carbon samples were added in the flaks. Kinetic adsorption experiments were carried out and aliquots were taken between 0 and 300 min. Aliquots were acidified with concentrated nitric acid and then sent to the laboratory for As and Pb analyses. The results were processed and the removal (%) of As and Pb was calculated.

Results

Result 1

All the prepared activated carbons were granular. Despite the same initial particles size of the raw materials, the particles sizes of the prepared activated carbons are different depending on the type of raw material. The granular structure of the produced activated carbons is important due to the fact that these materials should be directly used for designing a water treatment unit. Using the granular activated carbon in water and wastewater treatment applications reduces the loss of material and enhances the recovery and the regeneration of adsorbents during the post-treatment.

It is worth to discuss the aspect of large-size compact particles in the prepared activated carbons. Nieto and Rangel studied [2], using an environmental scanning electron microscope, the $ZnCl_2$ activation mechanism during the activation and carbonization of agave bagasse. They identified that a molten phase is involved during these processes. That plastic phase might be responsible for the formation of $ZnCl_2$-activated carbon of compact large particles, which makes this type of activation favorable with concerning its application.

The ash content (Table 1) in the prepared activated carbons indicated a high content of impurities in the surface of the activated carbons, mainly evolved from impurities of the chemical activator, which remains on the surface after the catalyst washing step. It is necessary to improve the washing step increasing the concentration of HCl solution and increasing the amount of water during this step.

Table 1 Proximate analysis of the used raw materials

Raw material	Proximate analysis (wt.%)		
	Moisture	Dry matter	Ash(%)
RMS-RM	15.8	84.2	38.8
GS-RM	28.7	71.3	10.0
MSEP-AC	9.5	90.5	60.8
MSIP-AC	15.9	84.1	37.5
CPH-AC	4.9	95.1	9.5
CH-AC	17.2	82.8	32.9
CC-AC	10.3	89.7	19.6

(*) in dry basis

Result 2

In Figure 2 the nitrogen adsorption-desorption isotherms of the prepared activated carbons are shown and Table 2 shows the textural properties of the activated carbon calculated with the physisoption nitrogen data.

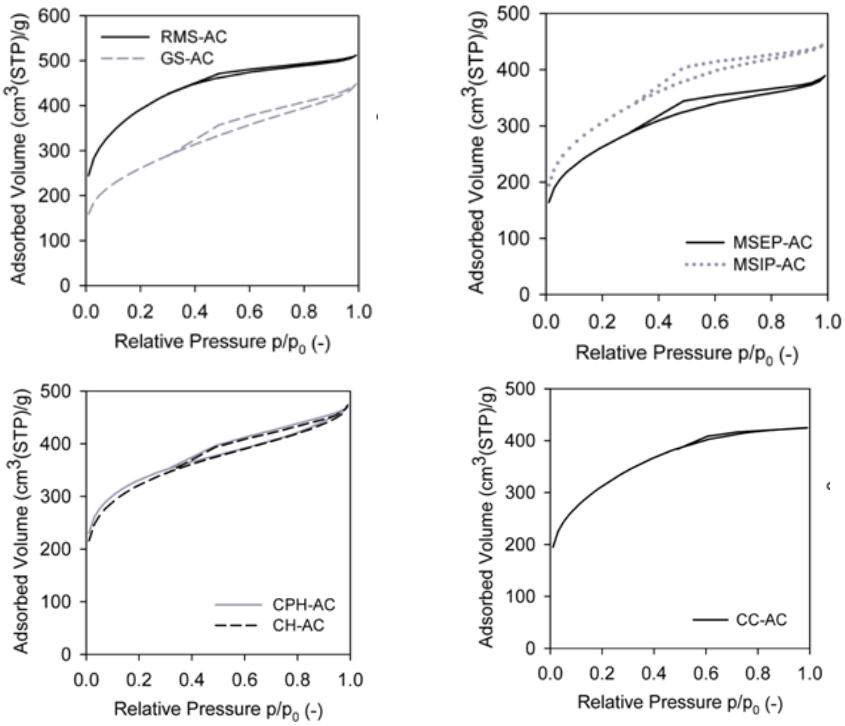

Fig. 2. Measured nitrogen adsorption-desorption isotherms of produced activated carbons.

The shape of nitrogen adsorption-desorption isotherms of the prepared activated carbons in this study (Fig. 2) corresponds basically to the type I isotherm according to the IUPAC classification [3], typical for microporous materials. Besides that the isotherms include hysteresis loops at higher relative pressures, which are typical for the IV type IUPAC isotherm, indicating the presence of a mesoporous structure. According to Fig. 2 and Table 2, all activated carbons produced from lignocellulosic agro-industrial wastes exhibit a well-developed microporous-mesoporous structure.

Table 2 Textural properties of the produced activated carbons.

Activated carbon	S_{BET} (m^2/g)	S_{meso} (m^2/g)	V_{micro} (mm^3_{liq}/g)	V_{net} (mm^3_{liq}/g)	V_{micro}/V_{net} (%)	C_{modif} (-)
RMS-AC	1405	965	214	792	27	45.0
GS-AC	937	766	82	693	12	68.7
MSEP-AC	939	504	221	602	37	19.0
MSIP-AC	1094	561	266	691	38	19.0
CPH-AC	1162	503	322	726	44	23.9
CH-AC	1135	518	305	732	42	20.8
CC-AC	1121	618	250	657	38	21.5

Result 3

Based on the FE-SEM images of ACs (Fig. 3) it is possible to see pores with different sizes, including smaller pores inside the larger ones. This shows that in the adsorption process, the access to the porous structure might be available for pollutants dissolved or carried by water or wastewater. The nice channel-like mesoporous-macroporous structure is visible for CC-AC (Fig. 3e). Otherwise, in other cases the pores are irregular, not perfectly circular and heterogeneous with different sizes. Some impurities were identified in the SEM images, specifically the white material on the activated carbon surface. This originates from the chemical activator and other activation and pyrolysis by-products.

Al ACs have the ability to adsorb methylene blue in solutions, however the CC-AC has the best adsorption activity, which is related to the higher pore volume according to the nitrogen isotherms (Fig. 2).

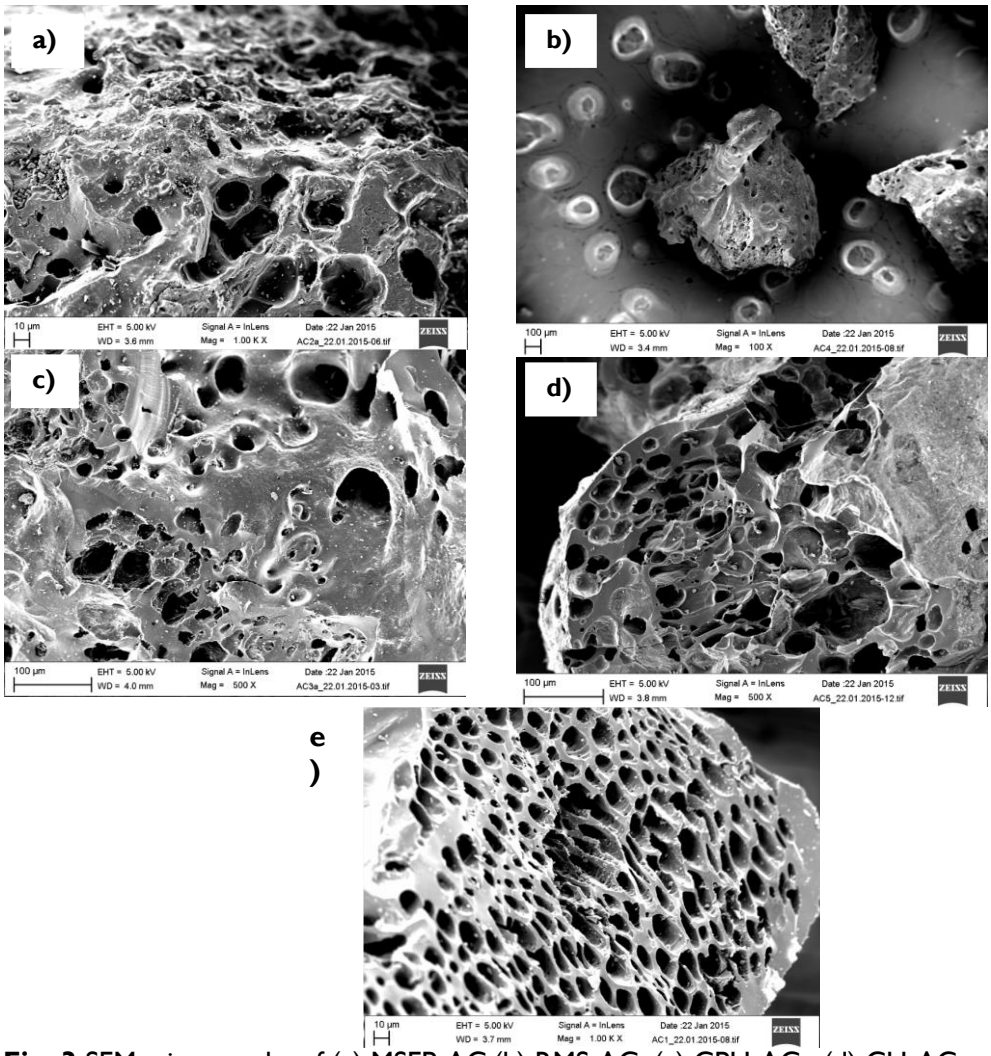

Fig. 3 SEM micrographs of (a) MSEP-AC,(b) RMS-AC, (c) CPH-AC , (d) CH-AC and (e) CC-AC.

Result 4

The adsorption experiments of the prepared activated carbons using methylene blue (MB) is shown in Fig. 4. From these results were determined the pseudo-second-order kinetic constants for methylene blue adsorption and is shown in Table 3.

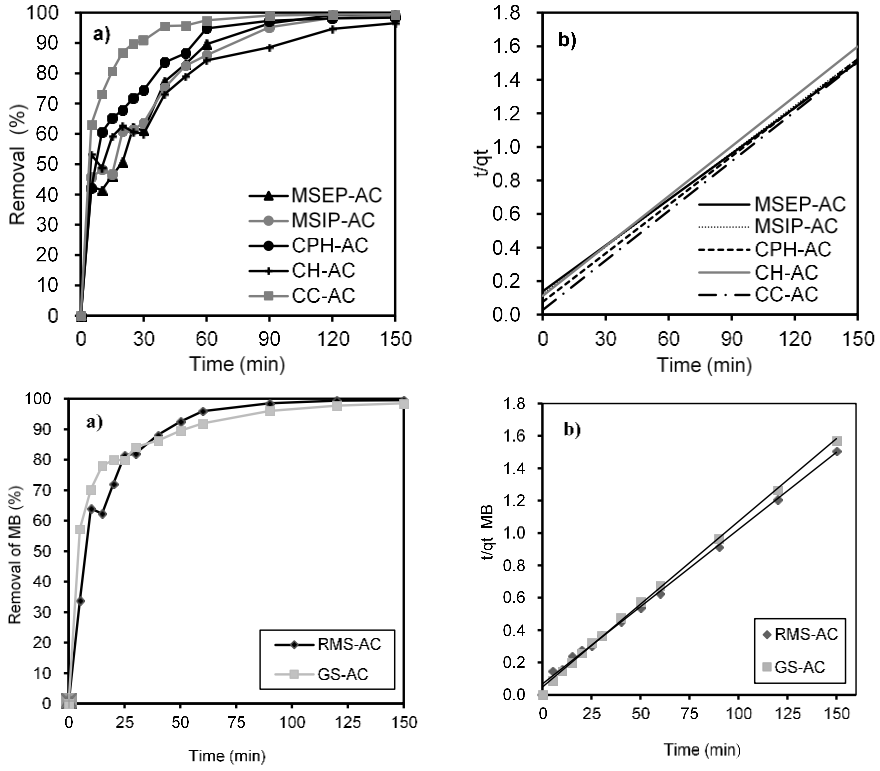

Fig. 4 (a) Removal of methylene blue using the individual produced activated carbons. (b) Pseudo-second-order kinetic plots for methylene blue adsorption by preöpared activated carbons.

The fact that the activated carbons perfectly follow the pseudo-second-order model (Fig. 4b, Table 3) shows that the adsorption between adsorbate and adsorbent is chemical in nature. Chemisorption involves valence forces through sharing or exchange of electrons between the sorbent and the sorbate [4].Thus, the different equilibrium adsorption capacities of investigated ACs may be a consequence of different surface properties (*e.g.* functional groups such as carbonyl or carboxyl groups which may be present).

Table 3 Pseudo-second-order kinetic constants for methylene blue adsorption.

Activated Carbon	R^2	q_e (mg/g)	k_2 (g/mg·min)	h (mg/g·min)
RMS-AC	0.9968	105.26	0.0013	14.86
GS-AC	0.9859	98.04	0.0020	20.96
MSEP-AC	0.9814	109.89	0.0006	7.23
MSIP-AC	0.9859	106.38	0.0007	8.10
CPH-AC	0.9956	104.17	0.0012	13.12
CH-AC	0.9858	101.01	0.0009	8.96
CC-AC	0.9995	102.04	0.0034	35.84

Result 5

The three samples of ACs CC-AC, MSEP-AC and CH-AC showed a high level of As and Pb removal compared with the commercial Chemviron, reaching very fast levels higher than 90% in just a few minutes of experiments. High surface area of the activated carbon is one of the reasons for that; however analysis of surface composition will be necessary to find further explanation.

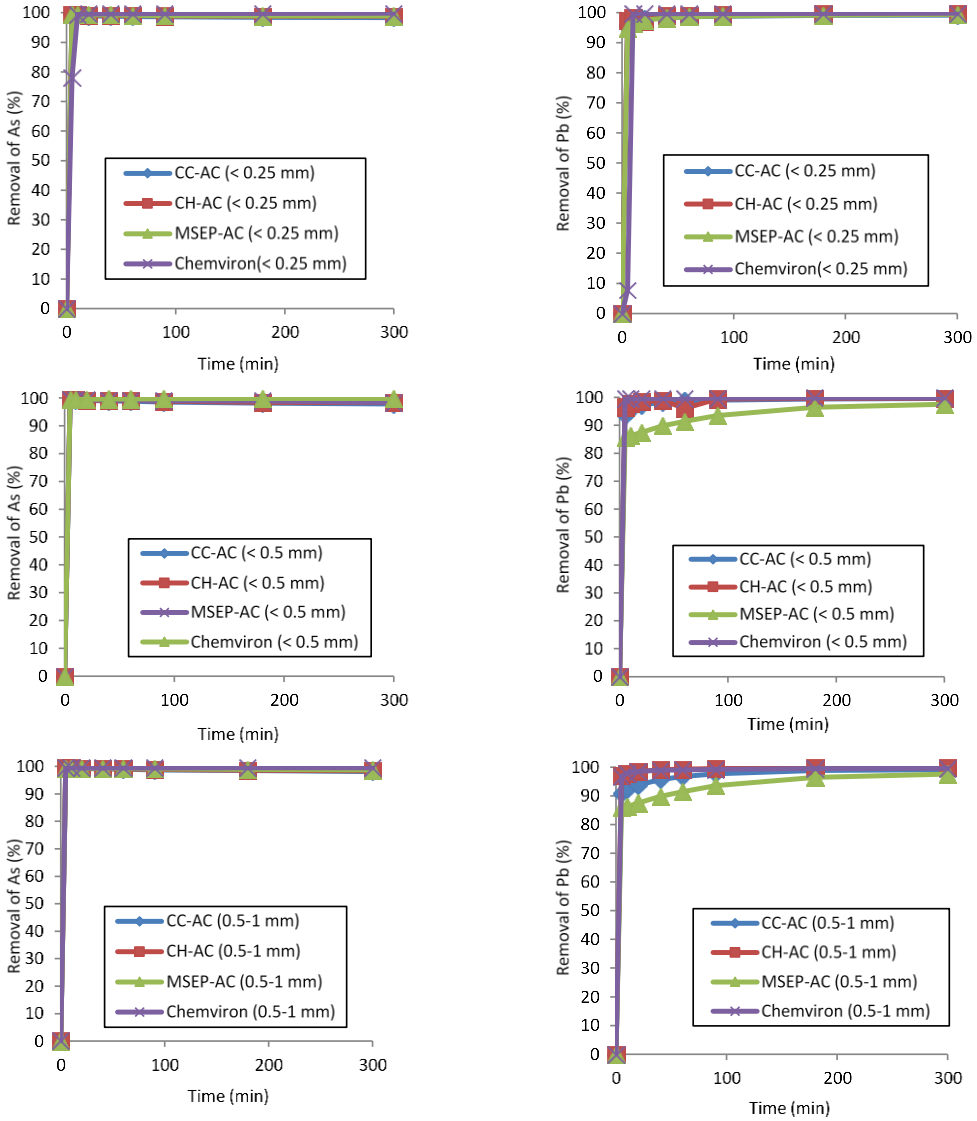

Fig 5. Removal of arsenic and lead from the river water by agrowastes based activated carbons and a commercial activated carbon according different particle size.

Relevance of the research

Different agrowastes were successfully used as precursors for activated carbon preparation with high surface area and micro-mesoporous structure. Agrowaste based activated carbons were efficient adsorbents for methylene blue in aqueous solutions and for As and Pb from the real Tumbes River water. Thus, agrowaste based activated carbons could be used as potential adsorbents for water and wastewater treatment.

Acknowledgements

The financial supports of the Finnish Funding Agency for Innovation (Tekes) (HYMEPRO project, reg. No. 40262/11), the Academy of Finland (AdMatU Project), the Academy of Sciences of the Czech Republic and Consejo Nacional de Ciencia, Tecnologia e Innovación Tecnológica (CONCYTEC) in Peru (joint project reg. No. 002/PE/2012) are gratefully acknowledged.

References

1. Cruz G, Pirilä M, Huuhtanen M, Carrión L., Alvarenga E & Keiski RL (2012) Production of activated carbon from cocoa (***Theobroma cacao***) pod husk. J. Civ. Environ. Eng. 2 (109) 1-6.
2. Nieto-Delgado C. & Rangel-Mendez JR (2013) *In situ* transformation of agave bagasse into activated carbon by use of an environmental scanning electron microscope. Microporous Mesoporous Mater. 167, 249-253.
3. Gregg SJ & Sing KSW (1982) Adsorption. Surface Area and Porosity. Academic Press, New York.
4. Ho YS, & McKay G (1999) Pseudo-second order model for sorption processes. Process Biochem. 34(5) 451-465.